BULLETIN N° 173
ACADÉMIE EUROPEENNE INTERDISCIPLINAIRE DES SCIENCES

lundi 4 mars 17h Maison de l'AX 5 rue Descartes 75005 Paris

"La matière organique insoluble dans les météorites carbonées et les roches archéennes"

Conférence de Sylvie DERENNE, Directrice de Recherche CNRS
Directeur-adjoint de l'UMR 7618 du CNRS : BioEMCo
Biogéochimie et écologie des milieux continentaux
Responsable de l'équipe de l'UMR 7618 localisée sur le site de Jussieu
"*Géochimie Organique et Minérale de l'Environnement*" (GOME)

Prochaine séance :
lundi 8 avril à 17h Maison de l'AX 5 rue Descartes 75005 Paris

1ère partie : Conférence de Nicolas PRANTZOS, Astrophysicien, Directeur de recherche au CNRS
Institut d'astrophysique de Paris (IAP), UMR 7095/UPMC et CNRS
« *Nucléosynthèse: l'origine des éléments chimiques dans l'Univers* »
2ème partie: Exposé de notre Collègue Michel GONDRAN,
ancien Conseiller scientifique de EDF/ Université Paris-Dauphine
« ***Le principe de moindre action interprété par la nature et par l'observateur en mécanique classique*** »

ACADEMIE EUROPEENNE INTERDISCIPLINAIRE DES SCIENCES
FONDATION DE LA MAISON DES SCIENCES DE L'HOMME

mars 2013

N°173

TABLE DES MATIERES

Prochaine séance:
lundi 8 avril à 17h Maison de l'AX 5 rue Descartes 75005 Paris

1ère partie: Conférence de Nicolas PRANTZOS, Astrophysicien, Directeur de recherche au CNRS
Institut d'astrophysique de Paris (IAP), UMR 7095/UPMC et CNRS
« *Nucléosynthèse: l'origine des éléments chimiques dans l'Univers* »

2ème partie: Exposé de notre Collègue Michel GONDRAN,
ancien Conseiller scientifique de EDF/ Université Paris-Dauphine

« Le principe de moindre action interprété par la nature
et par l'observateur en mécanique classique »

ACADEMIE EUROPEENNE INTERDISCIPLINAIRE DES SCIENCES
Fondation de la Maison des Sciences de l'Homme, Paris.

Séance du

Lundi 4 mars 2013

Maison de l'AX 17h

La séance est ouverte à 17h sous la Présidence de Victor MASTRANGELO et en la présence de nos collègues Gilbert BELAUBRE, Gilles COHEN-TANNOUDJI, Françoise DUTHEIL, Michel GONDRAN, Irène HERPE-LITWIN, Jean SCHMETS.

Etaient excusés François BEGON, Bruno BLONDEL, Michel CABANAC, Alain CARDON , Daniel COURGEAU, Claude ELBAZ Jean -Pierre FRANCOISE , Robert FRANCK, Walter GONZALEZ, Saadi LAHLOU,Gérard LEVY, Jacques LEVY , Valérie LEFEVRE-SEGUIN , Pierre MARCHAIS, Emmanuel NUNEZ, Pierre PESQUIES, Alain STAHL.

La séance est dédiée à la conférence de Sylvie DERENNE et au traitement de quelques projets internes de l'AEIS.

A) Le Président Victor Mastrangelo nous donne quelques éléments du CV de notre conférencière.

Sylvie DERENNE est Directeur de Recherche de 1ère classe de catégorie 1 au CNRS. Elle dirige l'équipe "Géochimie Organique et Minérale de l'Environnement" (GOME) de l'UMR 7618 BioEMCO de l'Université Pierre et Marie Curie (Paris 6).

Ancienne élève de l'ENS de Fontenay aux Roses , agrégée de physique option:chimie, docteur de l'Université Paris 6 elle possède depuis 1994 une habilitation à diriger des recherches. Elle est Directeur de Recherche au CNRS de 1ère classe de catégorie 1 depuis 2008 et Responsable de l'UMR 7618 BioEMCo.à Jussieu depuis 2006.

Chevalier de la Légion d'Honneur (2010), elle est par ailleurs, entre autres lauréate du Prix Grammaticakis-Neumann (Chimie) de l'Académie des Sciences (2009)

Elle est auteur de plus de 180 publications de rang A et de plus de **210** communications orales (congrès internationaux, conférences invitées). Parmi ses activités récentes, elle est entre autres membre scientifique de divers organismes: groupe Exobiologie du CNES, Programme National de Planétologie, Programme « **Physico-chimie du milieu interstellaire** ». Depuis 2011 elle est membre du Directoire de la Recherche de l'UMPC et depuis 2012 elle est Membre de la Commission scientifique "Systèmes écologiques" de **l'IRD (CSS3).**

B) Conférence de Sylvie DERENNE: LA MATIÈRE ORGANIQUE INSOLUBLE DANS LES MÉTÈORITES CARBONÉES ET LES ROCHES ARCHÉENNES

Les principaux objets d'étude sont **I**) les **météorites carbonées** (**Orgueil, 1864, Kainsaz, 1937, Murchison, 1969**, Tagish Lake, 2000) et **II)** les **Roches archéennes** très anciennes trouvées dans les sites **Warrawoona,** Australie,(3,5 milliards d'années), Middle Marker, Afrique du Sud,(3,4 milliards d'années),Buck Reef, Afrique du Sud,(3,3 milliards d'années), Josefsdal, Afrique du Sud, (3,3 milliards d'années), Gunflint, Canada, 1,9 milliards d'années.
L'**intérêt des météorites carbonées** réside dans les faits suivants:

- Elles comportent entre 1 et 4 % de matière carbonée majoritairement sous forme de Matière Organique (80 %) et non de type graphite ;
- Il s'agit de **Matière Organique extraterrestre** (intérêt en exobiologie) ;
- on y a détecté la **présence d'acides aminés dans la fraction soluble ;**
- on y cherche un Précurseur possible pour les premières formes de vie ;
- Il est intéressant de comprendre comment s'est formée cette Matière Organique (**MO)** ;

⇒**on peut ainsi y trouver des informations sur l'histoire des molécules organiques du système solaire et y rechercher des signatures extraterrestres** (matière absente des roches terrestres) .

Par ailleurs, **elles comportent des acides aminés dans leur fraction soluble ce qui pourrait évoquer une origine extraterrestre (***mais celle-ci peut résulter d'une contamination d'où l'étude de la matière insoluble***.)**

L'intérêt des roches archéennes tient au fait qu'elles comportent des traces de carbone (≈ 100 ppm) et, parmi les éléments figurés, l**es plus anciennes formes de vie sur terre**

On étudie la MO Insoluble (MOI) par ce qu'elle est la plus abondante et **la moins affectée par des risques de contamination** alors qu'existe une contamination possible, après dépôt, de la fraction soluble qui, toutefois n'affecterait pas les structures liées par liaison covalente au kérogène[1].

Les principales difficultés dans l'étude de la **MOI** sont liées à la **nécessité** d'**isoler la MOI associée à la matrice minérale**. On peut schématiser ainsi les démarches à partir d'une roche totale **broyée**:

ROCHE TOTALE BROYEE
↓

Composés solubles	↓	**Extractions (eau et solvants)**
Composés hydrolysables	↓	**hydrolyse basique(KOH/CH3OH)**
déminéralisation	↓	**hydrolyse acide (HCl)**
	↓	**Traitement (HF / HCl)**
	↓	**Extractions (solvants)**
	MOI +minéraux réfractaires (8 – 20 %)	

[1] Le **kérogène**, du grec signifiant *qui engendre la cire*, est la substance intermédiaire entre la matière organique et les combustibles fossiles.

Comme elle est **chimiquement inerte**, il est nécessaire de **combiner les outils analytiques**. L'approche analytique est fondée sur les méthodes suivantes:

- **spectroscopiques:** ***Infrarouge à transformée de Fourier (IRTF)***, ***Résonance magnétique nucléaire à l'état solide*** **(RMN ^{13}C, ^{15}N)**, ***Résonance paramagnétique électronique*** (**RPE**) (radicaux)-
- **dégradations thermiques** - ***pyrolyses, méthylation*** - ou **chimiques** - ***oxydation au RuO_4***,(tétra-oxyde de ruthénium)-chromatographie gazeuse du pyrolysat,
- **microscopiques** - ***Microscopie électronique en transmission à haute résolution (METHR ou HRTEM)***
- **Isotopiques** - dosage de δ^{13}C, δ^{15}N, δ D

Résultats Analytiques

I) LA MATIERE ORGANIQUE INSOLUBLE DES MÉTÉORITES CARBONÉES (plus particulièrement sur Orgueil et Murchison)

1°) Spectroscopie RMN

La spectroscopie par RMN ^{13}C et ^{15}N a révélé un caractère aromatique fort (cyclique) avec de l'azote hétérocyclique sans précurseur d'acides aminés.et un rapport CH_3 / CH_2 traduisant un **degré de ramification élevé des chaînes**. **Ceci est analogue à ce qu'on trouve dans le milieu interstellaire**, mais malheureusement 30 % des carbones ne sont pas détectés par RMN.

Par ailleurs la RMN ne donne que le **nombre d'unités aromatiques et non leur taille** d'où la nécessité de mettre en œuvre d'autres méthodes d'investigation.

2°) **Microscopie électronique en transmission à haute résolution (METHR ou) pour mesurer la taille des molécules**

Celle-ci révèle:

- **des unités aromatiques de petite taille traduisant un faible degré d'organisation contrairement au milieu interstellaire.**

Ceci pose le problème de l'**origine des chaînes aromatiques**:

- dans le milieu interstellaire, les plus petites unités sont détruites par photodissociation alors qu'elles sont protégées dans les météorites. **La distribution des météorites pourrait être originelle, tandis que la distribution interstellaire en petites molécules résulterait de la destruction des molécules.**

La taille des unités aromatiques retrouvées (en nombre de cycles benzéniques) est en **faveur d'une origine possible commune avec le milieu interstellaire.**

3°) Résonance paramagnétique électronique (RPE) et dégradations thermiques. recherche de signatures extra-terrestres - Comparaison avec le milieu terrestre.

La mesure des temps de relaxation en RPE est également favorable à des signatures extra-terrestres en mettant en évidence une **distribution différente (hétérogène) des radicaux** par rapport au milieu terrestre. La dégradation thermique montre par exemple la présence **de di-radicaux absents dans le milieu terrestre** .En milieu terrestre, existe une augmentation de la taille des unités polyaromatiques ce qui est contraire aux météorites.

La **pyrolyse** avec étude par **chromatographie en phase gazeuse** met essentiellement en évidence des unités aromatiques, des hétéro-éléments et une **grande diversité d'isomères**. La pyrolyse / CG / SM ne donne que peu d'informations sur les unités polaires et les chaînes aliphatiques (**Pas de trace de composés aliphatiques présents en RMN**). Elle permet néanmoins de détecter des fonctions esters/éthers.

L'oxydation au Ruthénium (RuO4) met en évidence **des chaînes aliphatiques courtes hautement ramifiées avec un fort taux de réticulation**. La pyrolyse permet également de détecter des produits soufrés (Thiophènes mais sont-ils préexistants?) On trouve du Soufre Organique par la méthode XANES (Spectroscopie de structure près du front d'absorption de rayons X) :

Les figures ci-dessous résument les résultats obtenus sur les structures moléculaires par différentes techniques: RMN, XANES, HRTEM (Microscopie Electronique en Transmission à Haute Résolution), Pyrolyse et enrichissement au Deutérium.:

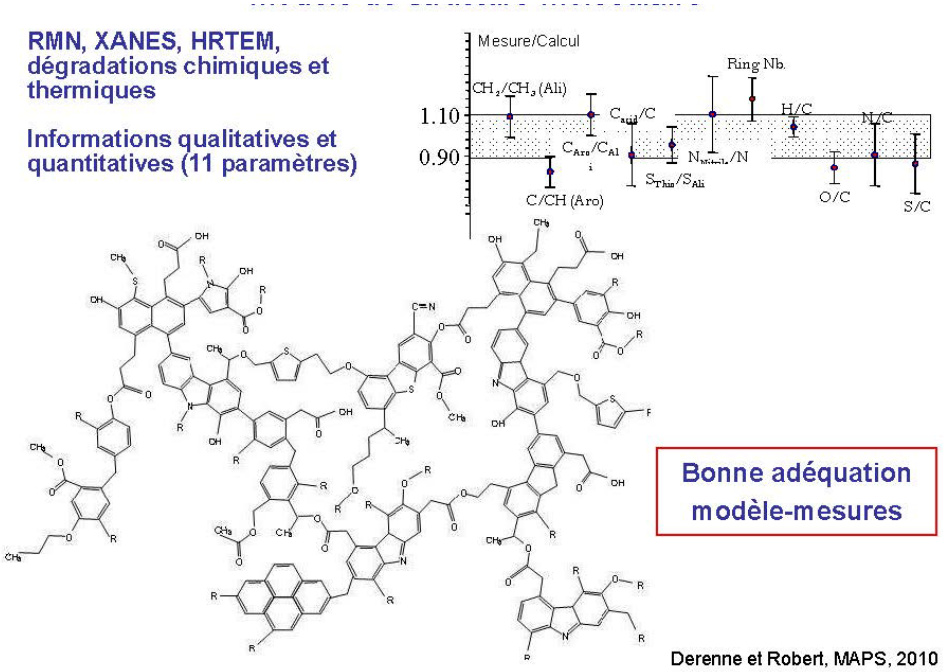

Figure 2:Modèle de Structure moléculaire

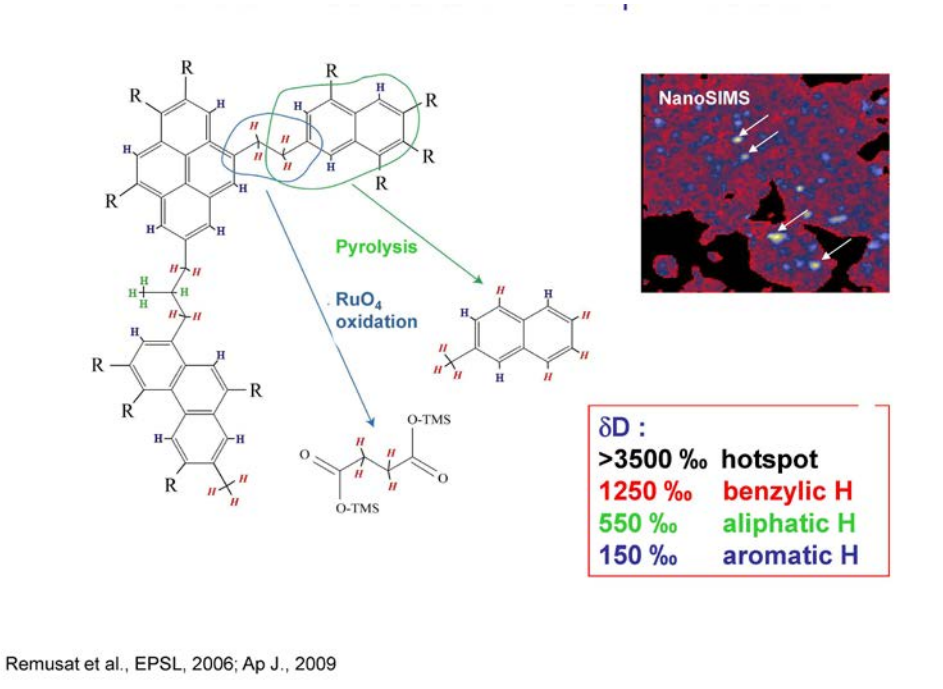

Figure 3 : Enrichissement au Deutérium: isotopie moléculaire

La MOI se serait t enrichie en deutérium après sa formation par échange avec un gaz riche en D en présence de rayonnement UV. Il existe trois types d'Hydrogènes enrichis au Deutérium: aromatiques (les moins abondants), aliphatiques (plus abondants), benzéniques (prédominants avec liaison C-H faible) . L'enrichissement en De lié à une faible énergie de la liaison C-H, **aurait eu lieu après sa formation**. **Ceci irait à l'encontre d'un héritage interstellaire.**

Les démarches analytiques ci-dessus ont donc mis en évidence pour la **MO insoluble des météorites carbonées** une bonne connaissance de leur structure chimique, une mise en évidence de signatures extraterrestres; elles suggèrent qu'un mécanisme de formation de la MO prendrait place dans le disque de poussières et de gaz avec un enrichissement en deutérium après sa formation.

II) LA MATIÈRE ORGANIQUE DES CHERTS[2] ARCHÉENS (Warrawoona)

Les roches de Warrawoona seraient vieilles de 3,5 milliards d'années. Selon une première théorie (Schopf,1993), **la matière organique y aurait une origine de microfossiles -bactéries filamenteuses -.**. Une théorie plus récente (Brasier et al., 2002; Garcia-Ruiz et al., 2003) **remet en cause cette interprétation**. Cette divergence d'interprétation a conduit à pratiquer plusieurs analyses analytiques et pyrolytiques pour essayer de valider l'une ou l'autre hypothèse.

Après un traitement analogue à celui des météorites, on a observé un caractère aromatique en accord avec une certaine maturité , un important taux de chaînes aliphatiques, un spectre de RMN et IRTF très différent de celui de simples kérogènes et montrant également la présence de chaînes aliphatiques. **L'ensemble des explorations - y compris l'analyse chimique - ont donné des résultats en faveur d'une biosynthèse**.

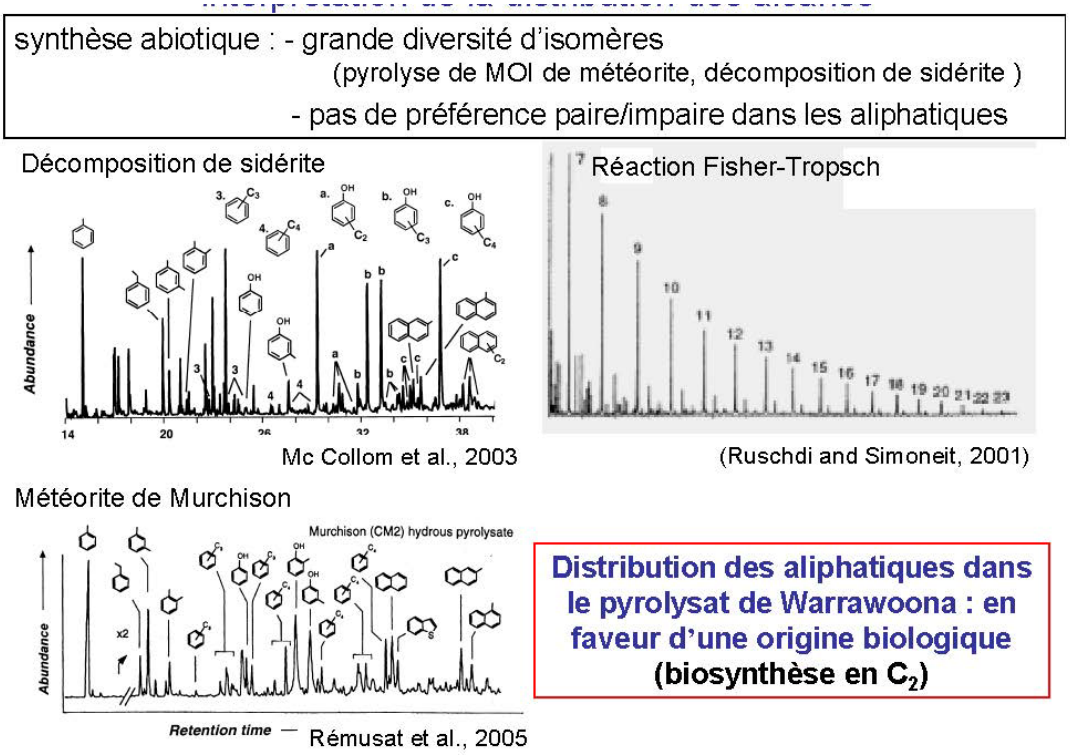

Figure 4 : Interprétation de la distribution des alcanes

[2] Chert: roche siliceuse

Il s'en suit que pour les **MO des cherts archéens,** ces méthodes analytiques mettent en évidence une **biogénicité** (marqueurs si composante aliphatique suffisante) et une **syngénicité** (outil basé sur la forme de raie RPE).

C) PROJETS INTERNES AEIS

1) **Notre Président nous exprime la satisfaction qu'il a éprouvée lors de sa visite auprès de nos Collègues de Nancy. Un rapprochement entre Paris et Nancy serait très utile en vue de colloques et de publications.**
2) **le 8 avril 2013 une réunion du comité scientifique se tiendra avant l'arrivée du Conférencier en vue de la préparation du futur Colloque.**
3) **Le 6 mai 2013 s'orientera plus particulièrement vers des exposés des membres de l'AEIS**.

Après cette très riche conférence et l'exposé de nos futurs projets, notre séance prend fin,

Bien à vous

Irène HERPE-LITWIN

Comptes-rendus de la section

Nice-Côte d'Azur

Mais malheur à l'auteur qui veut toujours instruire. Le secret d'ennuyer est celui de tout dire !
Voltaire.

Compte rendu de la séance du 21 février 2013
(167ème séance)

Présents :

Richard Beaud, René Blanchet, Patrice Crossa-Raynaud, Guy Darcourt, René Dars, Jean-Pierre Delmont, François Demard, Pierre Gouirand, Jacques Lebraty, Maurice Lethurgez, Claude Nigoul, Maurice Papo.

Excusés :

Jean Aubouin, Pierre Bourgeot, François Cuzin, Yves Ignazi, Jean-Marie Rainaud.

1- Approbation du compte rendu de la 166ème séance.

Le compte rendu est approuvé à l'unanimité des présents.

2- Le mois écoulé.

Claude Nigoul aborde le problème du site Internet sur lequel se trouvent les textes des conférences que nous avons tenues ces deux dernières années au MAMAC et craint que celui-ci ne soit difficilement abordable.

Il suggère une autre solution plus facile d'accès, par *Géopolitis* dont il s'occupe. On pourrait aussi en créer un qui nous serait exclusif.

Ce problème a été déjà évoqué plusieurs fois sans que l'on ait trouvé de solution satisfaisante.

Notre confrère promet d'y réfléchir à nouveau et en profite pour suggérer que nous puissions avoir des membres correspondants de très haut niveau, extérieurs à Nice, auxquels nous ferions part de nos activités : réunions, conférences, publications.

3- Débat : *The digital natives* (Patrice Crossa-Raynaud**).**

Lorsque j'étais étudiant, après la guerre, nous passions des heures à prendre des notes manuscrites des cours « magistraux » de nos professeurs. On est ensuite passé aux polycopies.

Actuellement, tout cela est bouleversé car les étudiants actuels ne supportent plus les cours magistraux de deux heures car ils disposent tous d'ordinateurs portables où ils peuvent trouver tous les éléments qui constituent le cours magistral. Les étudiants actuels sont étonnamment habiles pour manipuler leurs

ordinateurs et à rechercher tout ce qui se rapporte au sujet traité, d'où le sobriquet affectueux de « *digital natives* ».

Mais si on sait profiter de leurs aptitudes, ces étudiants sont capables de performances et d'un enthousiasme surprenant.

Le problème pour les enseignants est donc d'arriver à motiver les étudiants. Pour cela, certains proposent aux étudiants de travailler le sujet de la prochaine conférence et ensuite d'établir un dialogue permettant d'approfondir le sujet avec eux, d'expliquer les parties difficiles et de repérer les informations fausses ou hasardeuses qui encombrent Internet.

En allant au bout de cette idée, l'Université de Stanford en Californie a mis un enseignement en ligne lorsque deux professeurs ont conçu un cours en accès libre sur « l'intelligence artificielle ». Il a attiré 150 000 étudiants du monde entier. Mais il s'agit d'un cas particulier qui ne s'applique pas à des étudiants de première année. Le taux d'abandon chez les étudiants va alors jusqu'à 90 % pour certains grands cours en ligne. Ils ne sont en outre pas du tout adaptés aux étudiants en difficulté.

René Blanchet : l'Académie des Sciences vient de rédiger un rapport : « L'enfant et les écrans » (voir le site de l'Académie des sciences, page d'accueil). Par ailleurs Michel Serre a publié un livre sur le sujet: « Poucette ».

Depuis très longtemps, il existe aux USA un type d'enseignement par petits groupes d'étudiants, sous forme de séminaires. L'ordinateur y règne en maitre.

L'ordinateur est aussi l'outil qui permet l'enseignement de masse ; cette évolution est inéluctable. Même dans nos facultés de médecine, où les effectifs de première année sont très élevés, l'enseignement a complètement changé et chaque étudiant prend ses notes sur ordinateur.

C'est un changement complet de l'enseignement qui est en cours. Il conduit en outre les étudiants à travailler plus facilement ensemble, ce qui sera le plus souvent le cas par la suite dans leur vie active.

Mais cela exige des enseignants un effort d'adaptation monumental.

Claude Nigoul : ainsi qu'il a été dit dans de nombreuses universités américaines, on s'inscrit à un (des) cours en ligne.

René Blanchet : il y a effectivement des universités comme Harvard, Stanford, MIT qui diffusent mondialement des cours en ligne (programmes MOOC). Cela commence en France (Rennes, ENS Lyon …) et va entraîner une révolution dans le fonctionnement de nos universités : droits d'inscription, validation des acquis, relations étudiants – professeurs etc. Cela permettra aussi de sensibiliser à l'excellence les meilleurs cerveaux d'autres pays du monde et impliquera une formation particulière des enseignants

Claude Nigoul : cela bouleverse complètement les logiques d'inscription aux universités où tout le monde peut s'inscrire.

René Blanchet : c'est, toutes proportions gardées, le principe du Collège de France. C'est l'accès en ligne à un enseignement de masse, donné par les meilleurs professeurs, et donc de grande qualité.

L'observatoire de la Côte d'Azur travaille à la mise au point d'un système comparable pour des cours de master et doctorat.

*o*o*o*o*o*o*o*o*o*o*o*o*o*o*o*o*o*o*o*o*o*o*o*o*o*o*o*o*o*o*o*o*o*o*o*o*o*o*o*o*o*o*o*o*o*o*o*o

Prochaine réunion
le jeudi 21 mars 2013 à 17 heures
au siège : Palais Marie Christine - 20 rue de France
06000 NICE

Prochaine conférence à la Bibliothèque Nucéra
Parking Promenade des Arts
le mercredi 27 mars 2013 de 17 à 19 heures
Professeur Pierre Coullet
"Un cercle pour décrire le monde"

Annonces

I. VISITE DE NOTRE PRESIDENT AUPRES DES COLLEGUES DE LA SECTION DE NANCY

Notre Président nous fait part du plaisir et de l'intérêt qu'il a portés à sa dernière visite auprès des membres de notre section de NANCY de l'AEIS. Il a trouvé la section fort active et prête à relever les défis qui nous attendent et se réjouit de les avoir trouvés si coopératifs.

II. PARUTION DU LIVRE DE NOTRE COLLEGUE Gilles COHEN-TANNOUDJI

Notre Collègue Gilles COHEN-TANNOUDJI nous fait part de la parution de son livre écrit en commun avec Michel SPIRO le 19 avril 2013:

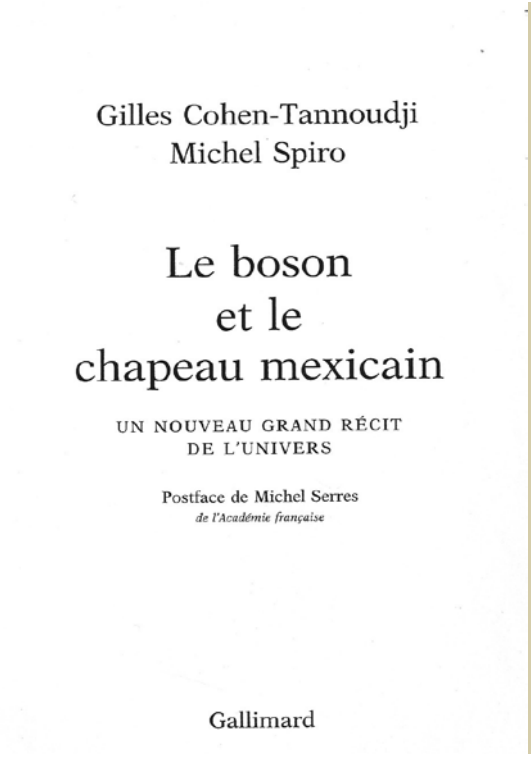

Le boson ? C'est l'ultime particule élémentaire prédite par la théorie de l'infiniment petit et qui manquait encore : postulée en 1964 par Robert Brout, François Englert et Peter Higgs, et appelée par simplification le «boson de Higgs», elle explique que le photon — particule qui transmet la force électromagnétique — n'a pas de masse, à l'encontre de celles véhiculant la force faible. Une telle dissymétrie était a priori incompatible avec la symétrie fondamentale, dite «de jauge», sur laquelle est fondé le modèle standard de la physique des particules.

Le chapeau mexicain ? C'est le mécanisme grâce auquel le boson dont la découverte, avec le grand collisionneur de hadrons du CERN, a été annoncée au monde entier le 4 juillet 2012, rend compte, en préservant les acquis du modèle standard, de l'origine des masses des particules élémentaires. Le boson et le chapeau mexicain se placent à la croisée — retracée par les deux auteurs en dialogue avec François Englert — des chemins de l'évolution des théories de l'astrophysique contemporaine et, sur près de trente années, d'une véritable aventure scientifique, technologique et humaine menée par le CERN, dont Michel Spiro fut le président du Conseil. Mais la particule observée a-t-elle les propriétés définies par le modèle standard, ou en possède-t-elle d'autres, prédites par des théories concurrentes des composants élémentaires de la matière? Faudra-t-il bientôt écrire encore un nouveau grand récit de l'univers ?

Une table détaillée des matières est accessible sur le site: http://www.gicotan.fr/images/table_des_matieres.pdf

III. SITE EUROPEEN CORDIS

Notre Collègue Jean SCHMETS en charge des relations avec l'Union Européenne nous fait part de colloques européens susceptibles de nous intéresser:

'International Workshop on Organic Matter Spectroscopy 2013', Lagarde, France
Date: 2013-07-16
Organiser: For further information, please visit: **http://woms13.univ-tln.fr/**
Summary: An '**International Workshop on Organic Matter Spectroscopy 2013**' will be held from 1**6 to 19 July 2013 in Lagarde, France**. Fluorescence spectroscopy is a type of electromagnetic spectroscopy which analyzes fluorescence from a sample.
Lien:
http://cordis.europa.eu/search/index.cfm?fuseaction=events.document&EV_LANG=EN&EV_RCN=35580&pid=0

Country: FRANCE

1st International Conference in Internet Science, Brussels, Belgium
The 1st International Conference in Internet Science, will be organized from April 10 to 11 in Brussels, under the aegis of the European Commission by the the EINS project, the FP7 European Network of Excellence in Internet Science **http://internet-science.eu**
Organisation: SIGMA ORIONIS
Country: FRANCE

New opportunities for 3D technology in medicine
Until now, physicians have largely been skeptical of the advantages of 3D technology.
But this may be about to change: the findings of a new study show that even experienced surgeons stand to benefit from the third dimension.
Organisation: Fraunhofer
Country: GERMANY

Hydra IX - The European Summer School on Stem Cell & Regenerative Medicine
Registration is now open for the eight Summer School in the highly successful Hydra series on Stem Cells and Regenerative Medicine. Deadline for applications is 03 May 2013
Organisation: Optistem
http://www.regonline.co.uk/Hydra2013
Country: UK

SPADnet, a New Concept for Biomedical Imaging, reaches its main intermediate milestone - SPADnet presents a comprehensive overview of its advances at London Image Sensors 2013
The SPADnet project – “Fully Networked, Digital Components for Photon-starved Biomedical Imaging Systems” – is coordinated by EPFL and it includes seven leading European experts in image sensors, medical imaging, and photonics. A comprehensive overview of its advances is scheduled to be presented at the London Image Sensors conference.
Organisation: Ecole Polytechnique Fédérale de Lausanne (EPFL)
Country: SWITZERLAND

AgedBrainSYSBIO, a medium-scale research initiative against neurodegenerative diseases
March 2013, Paris (France) - A European group of academic laboratories and industrial scientists from SMEs will combine integrative systems biology & comparative genomics for studying human brain ageing and/or most common age-related diseases with a special emphasis on late-onset Alzheimer Disease for identifying and validating new molecular targets and biomarkers.

Organisation: Inserm Transfert SA
Country: FRANCE

Workshop on “Electric Vehicle Batteries: Moving from Research Towards Innovation"
Within this joint workshop, to be held on 10 April 2013 in Brussels, the European Commission and the European Technology Platforms involved in the PPP European Green Cars Initiative, EPoSS and ERTRAC, wish to discuss current European activities and policies for bridging the gap between research and innovation in the domain of batteries for the electric vehicle.
Organisation: VDI/VDE Innovation+Technik
Country: GERMANY
Category: Event

Documents

Pour compléter la conférence de Mme Sylvie DERENNE, nous vous proposons le texte complet de deux articles écrits par Sylvie DERENNE et François ROBERT dont les résumés et introductions, traduits en français, vous avaient été communiqués dans le précédent bulletin.

p.16. *Model of molecular structure of the insoluble organic matter isolated from Murchison meteorite issu de* de *Meteoritics and Planetary Science 1-14(2010),*

p.27 *Molecular evidence for life in the 3.5 billion year old Warrawoona chert* issu de *Earth and Planetary Science Letters 272 (2008) 476–480*

Pour préparer la conférence de Nicolas PRANTZOS nous vous proposons d'aller consulter le site:

http://books.google.fr/books?id=IZzlF5DfjuQC&pg=PA15&lpg=PA15&dq=PRANTZOS+Nicolas+nucléosynthèse+stellaire

Pour préparer sa communication notre Collègue Michel GONDRAN, nous propose:

p. 32 un résumé de sa présentation

p. 33 The Euler-Lagrange and Hamilton-Jacobi actions and the principle of least action

p. 45 The principle of least action as interpreted by Nature and by the observer par Michel GONDRAN

The Meteoritical Society

Meteoritics & Planetary Science 1–14 (2010)
doi: 10.1111/j.1945-5100.2010.01122.x

Model of molecular structure of the insoluble organic matter isolated from Murchison meteorite

Sylvie DERENNE[1*] and François ROBERT[2]

[1]BioEMCo, UMR CNRS 7618, UPMC, 4 Place Jussieu, 75252 Paris Cedex 05, France
[2]Laboratoire d'Etude de la Matière Extraterrestre, UMS CNRS 2679 NanoAnalyses, Museum National d'Histoire Naturelle, 61 rue Buffon, 75005 Paris, France
[*]Corresponding author. E-mail: sylvie.derenne@upmc.fr

(Received 10 May 2010; revision accepted 28 July 2010)

Abstract–The molecular structure of the insoluble organic matter (IOM) from Murchison meteorite has been investigated by our group for several years using a large set of analytical methods including various spectroscopies (Fourier transform infrared spectroscopy, nuclear magnetic resonance, electron paramagnetic resonance, X-ray absorption near-edge spectroscopy), high resolution electron microscopy, and thermal (pyrolyses in the presence or not of tetramethylammonium hydroxide) and chemical (RuO_4 oxidation) degradations. Taken together, these techniques provided a wealth of qualitative and quantitative information from which we derived 11 elemental and molecular parameters on the same IOM residue. In addition to the basic elemental composition, these parameters describe the distribution of the different types of carbon, nitrogen, and sulfur atoms as well as the size of the polyaromatic units. We therefore propose for this molecular structure a model which fits with these 11 molecular quantitative parameters. Several cosmochemical implications are derived from this structure. Based on the fact that aromatic moieties are highly substituted and aliphatic chains highly branched, it can be anticipated that the synthesis of this IOM occurred through successive additions of single carbon units in the gas-phase ending by a spontaneous cyclization for chain length ≥7 C. As a whole, these observations favor of an organosynthesis in the Solar T-Tauri disk.

INTRODUCTION

Carbonaceous chondrites are known to contain substantial amounts (up to 4%) of organic matter, most of which occurs as insoluble organic matter (IOM). Numerous studies performed since the 1970s aimed at deciphering the chemical structure of this IOM, mostly in the Murchison meteorite. Indeed, a precise knowledge of the structure of the organic macromolecule contains irreplaceable information that traces its mechanisms of synthesis and its conditions of formation. During the last 10 yr, we have participated in this work, with the aim of reconstructing the overall molecular structure of Murchison IOM. This led us to propose a preliminary model (Rémusat et al. 2007). The latter was qualitative and limited to a small number of moieties and as mentioned by the authors themselves "to draw a molecular model should be the goal of a future work." The main weakness of this model structure appears to be the large size of the aromatic units which turns out to be impossible to balance with short aliphatic chains as required by molecular parameters. In this article, we propose such a more complete modeled structure that takes into account all these parameters.

The IOM, which constitutes more than 75 wt% of the bulk organic matter, is isolated from the bulk rock through water and solvent extractions to remove soluble organic compounds and successive HF/HCl treatments to dissolve most of the mineral matrix. Such acid treatments are known to not alter the IOM (Durand and Nicaise 1980). Acid insoluble residues are enriched in IOM but contain inorganic material mainly consisting of natural oxides, sulfides, and chlorides according to X-ray diffraction.

The chemical structure of IOM isolated from Murchison has been studied by both destructive and nondestructive methods. The former include thermal

M A P S | 1122-1349 | B | Dispatch: 18.10.10 | Journal: MAPS | CE: Vijay
Journal Name | Manuscript No. | Author Received: | No. of pages: 14 | PE: Karpagavalli

and chemical degradations followed by gas chromatography/mass spectrometry (GC/MS) (Studier et al. 1972; Lévy et al. 1973; Hayatsu et al. 1977, 1980, 1983; De Vries et al. 1993; Komiya and Shimoyama 1996; Sephton et al. 1998, 2000, 2004; Remusat et al. 2005a, 2005b; Huang et al. 2007; Yabuta et al. 2007) and the latter contain mainly spectroscopic techniques (nuclear magnetic resonance [NMR], Fourier transform infrared [FTIR] spectroscopy, X-ray absorption near-edge spectroscopy [XANES], and electron paramagnetic resonance [EPR]) along with high-resolution transmission electron microscopy (HRTEM) (Cronin et al. 1987; Ehrenfreund et al. 1992; Gardinier et al. 2000; Cody et al. 2002, 2008; Cody and Alexander 2005; Binet et al. 2002, 2004a, 2004b; Derenne et al. 2002, 2005; Yabuta et al. 2005; Wirick et al. 2006). Although each technique alone cannot provide definite information on the chemical structure of such a complex material, the combination of the results can be used to reconstruct the molecular structure of the IOM. However, quantitative data are key parameters to build up such a model and to assess its validity. Therefore, we will only use the studies reporting such parameters to construct the model and our qualitative observations will be used to support discussions. It is also important to note that variations in the bulk elemental compositions were reported in the literature (probably depending on the isolation procedures of the acid residues). To overcome this analytical bias, all the quantitative parameters used in the present work were obtained on the same residue, which contained 19% mineral matter (Gardinier et al. 2000).

The details of this structure reveal information of the conditions of the formation in space of the IOM. Therefore, the last section of the article discusses the possible organosynthetic pathways in the cosmochemical context of the formation of the solar system.

MODELING THE CHEMICAL STRUCTURE OF THE IOM

Analytical Constraints

Analytical methods including spectroscopic, microscopic, and degradation techniques were used to determine the analytical constraints that are discussed below. Experimental conditions for these methods were described in detail in the source papers; they are only briefly reported in the Appendix.

Aromatic Moieties

The elemental composition of the IOM isolated from Murchison point to a rather high aromaticity with hydrogen to carbon atomic ratios around 0.7 (Gardinier et al. 2000).

The aromatic nature of the IOM from Murchison was further evidenced by the occurrence of an intense band at 1600 cm^{-1} in its FTIR spectrum (Gardinier et al. 2000) and of a strong absorption at 285.5 eV in C-XANES, corresponding to the 1s-Π* transition of the aromatic carbons as in polyaromatic hydrocarbons (Derenne et al. 2002; Wirick et al. 2006; Cody et al. 2008). Moreover, a strong aromaticity was inferred from the pioneer solid-state ^{13}C NMR study, the Murchison IOM spectrum being dominated by a peak around 130 ppm in the (Cronin et al. 1987). Extensive CP/MAS ^{13}C NMR studies using variable contact time and IRCP sequence (Gardinier et al. 2000) and interrupted decoupling experiments (Cody et al. 2002) revealed that most of these aromatic carbons were nonprotonated, thus leading to two hypotheses: the polyaromatic units are either very large (hence a large number of nonprotonated core carbons) or, if smaller, they must be highly substituted. The HRTEM and EPR results reported below clearly support the second assumption.

In HRTEM, aromatic layers appear as fringes. Such layers can be isolated or stacked together to form coherent domains. Image analysis was developed to derive semiquantitative data from the HRTEM images (Rouzaud and Clinard 2002). In Murchison IOM, the distribution of the fringe lengths indicates that the aromatic layers in the meteorites are of rather small size, most of them exhibiting diameter between 0.25 and 1 nm, i.e., 1–4 ring large, the average values corresponding to two to three rings (Derenne et al. 2005). In addition, a relatively low level of organization is inferred from the rather high contribution of isolated fringes (65%). This is confirmed when coherent domains are considered as more than 70% of them are made up with only two stacked layers, nearly 30% comprising three layers. Finally, the average interlayer spacing is of 0.49 nm, i.e., far from graphite (0.3354 nm).

The occurrence of aromatic moieties was also inferred from chemical degradation studies, especially oxidations using trifluoroacetic acid, nitric acid, potassium dichromate, cupric oxide, or ruthenium tetroxide as reagents (Hayatsu et al. 1977, 1980; Remusat et al. 2005a, 2005b). However, the formation of benzene hexa- and tetracarboxylic acids was first considered to reveal the occurrence of highly condensed polyaromatic units (Hayatsu et al. 1977), but this interpretation was revisited (Hayatsu and Anders 1981). Indeed, the high degree of carboxylation of the aromatic oxidation products is also consistent with a high degree of substitution of the initial aromatic units. More recently, RuO_4 oxidation products pointed to less

condensed aromatic units in Murchison IOM than in high rank coals (Remusat et al. 2005a, 2005b). One- to four-ring aromatic products are extensively generated during pyrolyses with a lower abundance of the larger compounds (Studier et al. 1972; Hayatsu et al. 1977; Komiya and Shimoyama 1996; Sephton et al. 1998, 2000; Remusat et al. 2005b; Yabuta et al. 2007). As demonstrated by the above spectroscopic data, these aromatics are pre-existing in the IOM and thus are not mainly derived from secondary aromatization upon pyrolyses. Although the larger aromatics are the more difficult to detect upon GC/MS, the decrease of the abundance of the aromatic products when their size increases is consistent with the small size of the polyaromatic units derived from HRTEM. In addition, the presence of polyaromatic units containing pentagonal rings such as indene or acenaphthene was reported in several pyrolytic studies (Komiya and Shimoyama 1996; Sephton et al. 2000; Remusat et al. 2005b) and especially in Yabuta et al. (2007) although no quantification was performed and hence no relative abundance can be assessed for these compounds.

Aliphatic Linkages

Fourier transform infrared and ^{13}C NMR show that aliphatic carbons contribute along with aromatic ones to the molecular structure of the IOM. Based on the CH_2 to CH_3 ratio, both techniques point to a high branching level in the aliphatic chains (Ehrenfreund et al. 1992; Gardinier et al. 2000). A number of chemical degradations were performed on Murchison IOM as far back as 1977 using a wide range of reagents such as trifluoroacetic acid, nitric acid, dichromate, copper oxide, and ruthenium tetroxide (Hayatsu et al. 1977, 1980; Remusat et al. 2005a, 2005b). Nitric acid did not yield any aliphatic acid but benzene polycarboxylic acids with up to three carboxylic groups (Hayatsu et al. 1977). Oxidation with dichromate mainly resulted in the formation of aromatic acids but small amounts of aliphatic diacids (C_3–C_5) and monoacids (C_3–C_7) were also identified (Hayatsu et al. 1977), the diacids being also detected upon copper oxide oxidation (Hayatsu et al. 1980). Diacids were supposed to be derived from hydroaromatics with five- to six-membered rings (Hayatsu et al. 1977). In contrast, monoacids were considered to represent alkyl substituents or bridging groups between aromatic units. However, it was mentioned that acids lower than propionic were probably lost and that those with more than seven carbon atoms may have escaped detection due to their low-intensity molecular ion (Hayatsu et al. 1977). Trifluoroacetic acid also led to the formation of small amounts of aliphatic compounds (alkanes and alkenes, the latter being dominant), but their origin was not clear. As a result, little information on the aliphatic linkages can be derived from these chemical degradations.

In contrast, ruthenium tetroxide is a mild and selective oxidizing agent that preferentially destroys aromatic rings converting them into CO_2. The aliphatic and acyclic structures released appear as carboxylic acids. These carboxylic functional groups mark either points of attachment in the kerogen or positions of labile functional groups, such as carbon–carbon double bonds and ether links (Stock and Wang 1986). This method was shown to be especially efficient to investigate the aliphatic structures in kerogens (Boucher et al. 1990). This oxidation reveals the short length of the chains (less than three carbons for side chains born by aromatic moieties and from two to seven carbons for aliphatic bridges between aromatic units) (Remusat et al. 2005a, 2005b; Huang et al. 2007). The short length of these chains is consistent with the lack of *n*-alkane/*n*-alk-1-ene doublets upon pyrolysis GC-MS as they are usually detected for carbon numbers higher than eight. However, when gases released upon pyrolysis are studied, alkanes and alkenes from methane to C_4-compounds are indeed identified (Remusat et al. 2005b). Aliphatic linkages released through RuO_4 oxidation also exhibit a high branching level, with substitution by methyl or ethyl groups. These substitutions are randomized as there is an isomeric diversity. Moreover, the occurrence of aliphatic chains linking several aromatic units (Remusat et al. 2005a, 2005b) is consistent with the high degree of cross-linking evidenced by solid-state ^{13}C NMR.

Oxygen Localization

Besides carbon and hydrogen, oxygen is the most abundant element of the IOM. Spectroscopic analyses reveal several forms of oxygen-containing functional groups. Indeed, C-XANES spectra exhibit a strong absorption at 288.9 eV (Wirick et al. 2006). 1s-Π* transition of carbons in carbonyl groups is known to occur at approximately 289 eV but C–H* resonances typical of sp^3-coordinated carbons with a high content of hydrogen have been reported at 289.2 eV. The XANES peak in the meteorite spectra thus suggests the presence of oxygen-containing functions. Solid-state ^{13}C NMR confirmed the presence of low amounts of carbonyl groups (resonance at 200 ppm) and revealed substantial amounts of carbon linked to oxygen (as in ether or aliphatic alcohols, at 55 ppm) and involved in carboxylic groups (acids and/or esters, around 168 ppm) (Gardinier et al. 2000; Cody et al. 2002). The presence of these groups is further supported by a high yield in CO_2 and CO upon vacuum pyrolysis of the IOM. The production of these gases reflects

Table 1. Summary of the chemical and molecular parameters of Murchison IOM used to model the chemical structure.

	Parameter	Experimental value	Analytical techniques	Other literature data
1	Aliphatic CH_2/aliphatic CH_3	2.0 ± 0.2[1]	^{13}C NMR, FTIR	1.57–1.79[2]
2	Nonprotonated aromatic C/protonated aromatic C	2.80 ± 0.28[1]	^{13}C NMR	2.33[2]; 1.86–2.70[3]
3	Aromatic C/aliphatic C	3.0 ± 0.3[1]	^{13}C NMR	2.76[2]; 3.08–3.28[3]; 1.82–2.17[4]
4	Acid C/total C	0.070 ± 0.014[1]	^{13}C NMR	0.074[2]
5	Thiophenic S/aliphatic S	3.17 ± 0.31[5]	S-XANES	
6	N as nitriles/total N	0.15 ± 0.05[a][5]	^{15}N NMR	
7	Average number of rings (2-D)	2.3 ± 0.3[6]	HRTEM	
8	H/C	0.70 ± 0.04[1]	Elemental analysis	0.70[7–9]; 0.71[10]; 0.38[11]; 0.52[12]; 0.48[13]; 0.53[14]
9	O/C	0.22 ± 0.02[15]	Elemental analysis	0.16[b][7]; 0.12[10, 13]; 0.25[14]
10	N/C	0.03 ± 0.006[5]	Elemental analysis	0.031[7]; 0.027[10, 16]; 0.015[12]; 0.012[13]; 0.034[8]; 0.044[17]; 0.029[14]; 0.035[18]; 0.039[9]
11	S/C		Elemental analysis	0.021[10, 13]
	Small aromatic units		EPR, ^{13}C NMR, HRTEM	
	Short chains		^{13}C NMR, oxidation-GC-MS	
	Highly branched aliphatics		FTIR, ^{13}C NMR, oxidation-GC-MS	
	Highly substituted aromatics		FTIR, ^{13}C NMR, pyrolysis GC-MS	

Note: NMR = nuclear magnetic resonance; FTIR = Fourier transform infrared; XANES = X-ray absorption near-edge spectroscopy; HRTEM = high-resolution transmission electron microscopy; EPR = electron paramagnetic resonance; GC-MS = gas chromatography–mass spectrometry.

[1] Gardinier et al. (2000); [2] Cody et al. (2002); [3] Cody and Alexander (2005); [4] Yabuta et al. (2005); [5] Remusat et al. (2005b); [6] Derenne et al. (2005); [7] Hayatsu et al. (1977); [8] Komiya and Shimoyama (1996); [9] Yabuta et al. (2005); [10] Hayatsu and Anders (1981); [11] Robert and Epstein (1982); [12] Kerridge et al. (1987); [13] Zinner et al. (1988); [14] Cody et al. (2002); [15] Binet et al. (2002); [16] Alexander et al. (1998); [17] Pearson et al. (2000); [18] Sephton et al. (2003). 21, 22, 23 24, 25

[a]Value determined for Orgueil insoluble organic matter (IOM).

[b]Calculated by difference.

decarboxylation and decarbonylation reactions which take place upon heating (Remusat et al. 2005b). Oxygen-containing nongaseous pyrolysis products were also identified; in addition to phenol, they comprise various aromatic ketones. These products support the presence of phenolic ethers that were previously suggested based on CuO oxidation (Hayatsu et al. 1977) or hydrous pyrolysis (Sephton et al. 1998) although in the latter experiments, the oxygen atom might have originated from the reagent. However, as pyrolysis polar products are poorly detected using an apolar column in GC/MS, a specific method was developed: the pyrolysis in the presence of tetramethylammonium hydroxide (Challinor 1989).

Tetramethylammonium hydroxide is both a base and a methylating agent, cleavage of polar bonds is enhanced and pyrolysis products are methylated in situ. Using this technique, aromatic acid methyl esters were identified along with dimethyl esters of short-chain diacids, thus revealing the presence of ester linkages between aromatic moieties (Remusat et al. 2005b). When aliphatic linkages are considered, the most precise information on oxygen groups was provided by RuO_4 oxidation which released hydroxy- and carboxy esters, thus showing that ether and ester functional groups occur within these linkages (Remusat et al. 2005a, 2005b).

Sulfur Speciation

A number of sulfur-containing products are released upon pyrolysis of the Murchison IOM (Lévy et al. 1973; Komiya and Shimoyama 1996) in agreement with a substantial sulfur content in the IOM. This content largely varies in literature (Table 1). This probably reflects that, depending on the isolation procedure, elemental sulfur (S_8) is more or less eliminated. In the present model, we used the organic sulfur content determined by Hayatsu and Anders (1981).

All the sulfur-containing pyrolysis products comprise thiophene rings, but these rings can either be pre-existing or formed upon pyrolysis (Remusat et al. 2005b). To investigate this question, K-edge sulfur

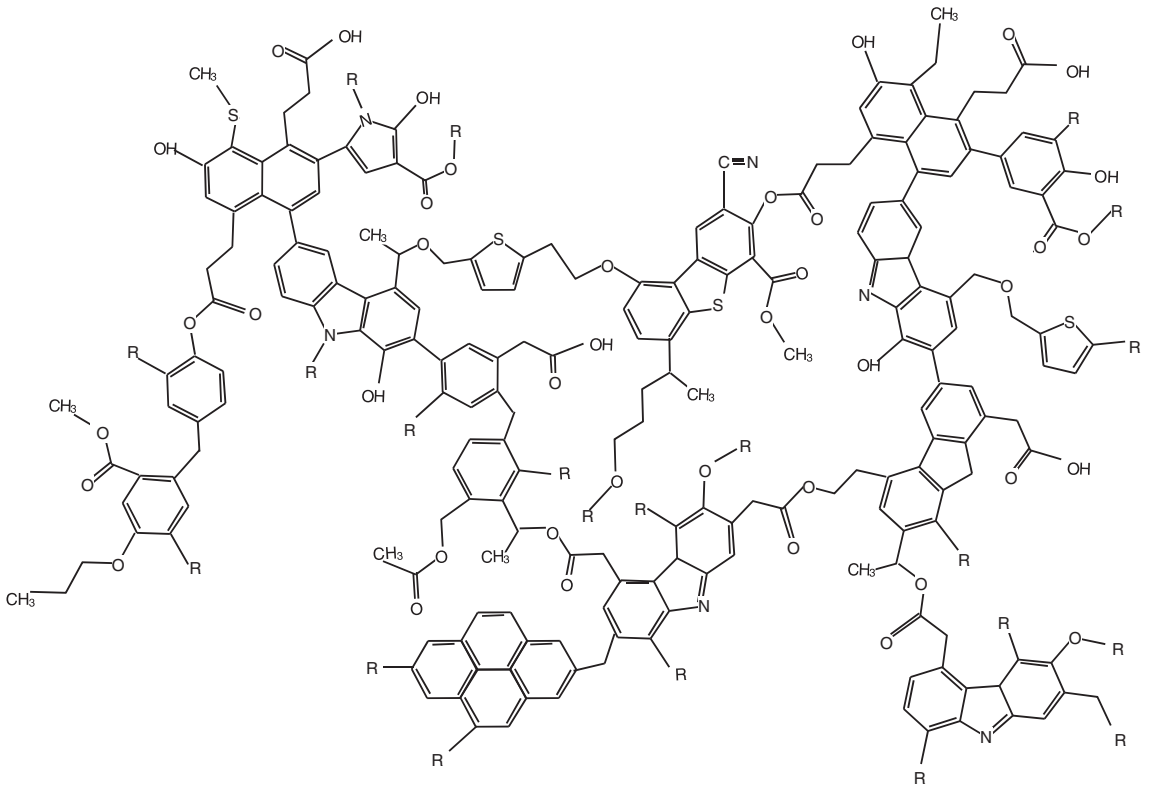

Fig. 1. Model of molecular structure of the insoluble organic matter of Murchison built from measured elemental and molecular parameters (cf. Fig. 2). R stands for an organic moiety.

XANES was performed on Murchison IOM revealing only 24% of the organic sulfur in thiophenes, the remaining 76% being in aliphatic sulfides (Derenne et al. 2002; Remusat et al. 2005b).

Nitrogen Speciation

Among heteroelements, nitrogen was also shown to occur in the IOM. A low amount of only one nitrogen-containing product, namely benzonitrile, could be detected in the pyrolysate from Murchison. The use of tetramethylammonium hydroxide did not improve such detection pointing to the lack (or at most very low contribution) of polar N-containing functions such as amide or amine. This was confirmed by solid-state ^{15}N NMR on Orgueil IOM which revealed that nitrogen is mainly involved in heteorocyclic units such as pyrroles. It must be noted that Orgueil led to the same results as Murchison when nitrogen products are considered. The lack of amide/amine functions was confirmed for Orgueil by solid-state ^{15}N NMR. The conclusions derived from Orgueil on nitrogen speciation probably also holds for Murchison The high thermal stability of these structures is in agreement with the lack of N-containing pyrolysis products and the release of N_2 only at high temperatures (900 °C) (Remusat et al. 2005b). A low contribution of nitrile groups can be put forward from the NMR spectrum of Orgueil IOM with a [Pyrrole N] to [Nitrile N] ratio being of approximately 5. No other occurrence for N (amide or amine) was detected with a detection limit of 5% relative to total N in the IOM.

Statistical Model of the IOM Structure

Taken together, the results derived from the different techniques described above led to a set of parameters that we used to build a model of molecular structure of the IOM. The 11 quantitative parameters that have been used are reported in Table 1. In this Table, for comparative purposes, we also report literature values of the same parameters obtained through elemental analysis and NMR on Murchison IOM samples isolated by other laboratories. The resulting structure (Fig. 1) accounts for molecular units (atoms or functional groups) whose abundance is higher than 3%. As a result, rare molecular occurrences are ignored to limit the structure around ≈200 carbon atoms. This does not affect the overall structure within the error bars assigned to each parameter. The adjustment between modeled and measured parameters is reported in Fig. 2, which shows that within ±10% the model fits all available data.

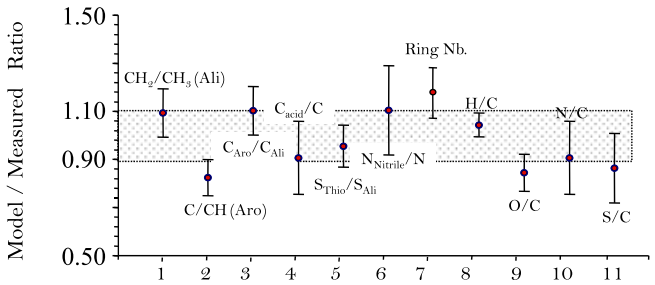

Fig. 2. Ratio of the values for the elemental and molecular parameters listed in Table 1 calculated from the modeled structure in Fig. 1 to those experimentally measured in the insoluble organic matter of Murchison.

It is worth noting that the quantitative data published in the literature on Murchison residues (Table 1) agree rather well with the presently used parameters. In particular, the fraction of aliphatic hydrogen was calculated as 0.70–0.74 by Cody and Alexander (2005) based on their ^{1}H NMR data. We have recalculated this parameter from the present model and obtain a value of 0.68 in good agreement with the aforementioned experimental value.

The present structure (Fig. 1) should be regarded as a statistical model and not as a unique solution that fits the measured parameters. Minor qualitative modifications such as position isomerism would also yield an acceptable structure. Note also that, because of its small size, this modeled structure cannot account for the large diversity of the products identified in pyrolysis and oxidation experiments.

Although the meteoritic IOM has been compared with terrestrial kerogens for a long time, it must be noted that the modeled structure is sharply different from what has been reported for kerogens and coals (Behar and Vandenbroucke 1986). Indeed, when immature terrestrial samples are considered, they contain long aliphatic chains with a low branching level in agreement with their biological origin. Such long aliphatic chains do not contribute to the IOM of meteorites. An increase in maturity in terrestrial samples induces the release of these chains hence not only an increase in aromaticity but also the increase in the size of aromatic moieties due to thermal annealing. In Orgueil, Murchison, and Tagish Lake meteorites, the size of the aromatic moieties remains small even when the aromaticity increases (Derenne et al. 2006). This is likely a consequence of the level of substitution which strongly differs between terrestrial materials and meteorites.

COSMOCHEMICAL IMPLICATIONS

This section is based on several specific features of the IOM. They are highlighted in Fig. 3 in so-called "regions of interest" (ROI noted **I–V**) of the modeled chemical structure.

Organics in Space

Organic molecules are found in a large diversity of astronomical environments. They are detected in stellar atmospheres, in dense and cool interstellar molecular clouds, and in circum-stellar disks associated with star formations. This organic matter comprises both a gaseous and a solid phase of nanometer dust particles (10–500 nm). In addition to the information derived from spectroscopy (temperature, density, and molecular species), theoretical simulations provide also a probe to the physical conditions where these molecules are formed because the rates of chemical reactions depend on time, temperature, and densities (Herbst and Millar 2008).

From the ISM to the T-Tauri Phase of the Sun

Sun-like stars form from the collapse of cold and dense "prestellar cores" ($n_H \approx 10^6$ cm^{-3}, $T \approx 10$ K) that hold a complex distribution of numerous organic species and dust. The populations of dust with their icy mantles are a vast reservoir of organic species. The resulting core becomes opaque and forms a so-called YSO (young stellar object) where the warm inner envelopes are heated by the central protostar ($n_H \approx 10^{7-8}$ cm^{-3}, $T \approx 100$ K) and where a complex organic chemistry is sometimes also observed (Ceccarelli 2004). Much of this matter is blown away and the newly born star starts its life as a T-Tauri star encircled by a dense protoplanetary disk. The average disk temperature is around 100 K, whereas the central regions, close to the star, where the telluric planets and the chondritic planetesimals formed, reach the vaporization temperature of refractory silicates and oxides (up to 2000 K) (Dullemond et al. 2002; Siebenmorgen and Krugel 2010).

As is obvious from this brief description, a profound evolution of the organic species can take place at each of the different stages of the formation of our own solar system (Herbst and van Dishoeck 2009). In this respect, the challenge of organic cosmochemistry is to provide a link between astronomical and chondritic observations.

In prestellar cores, the gas-phase chemistry is triggered by the presence of H_2. If the temperature exceeds the sublimation temperature of CH_4 or CO condensed on grains, chains of ion-molecule reactions starting with H_3^+ formed via $H_2 + H_2^+ \rightarrow H_3^+ + H$, lead to a variety of complex organic molecular ions (Herbst and Wakelam 2008; Woodall et al. 2008). As a result of the processes involved in this type of ionic

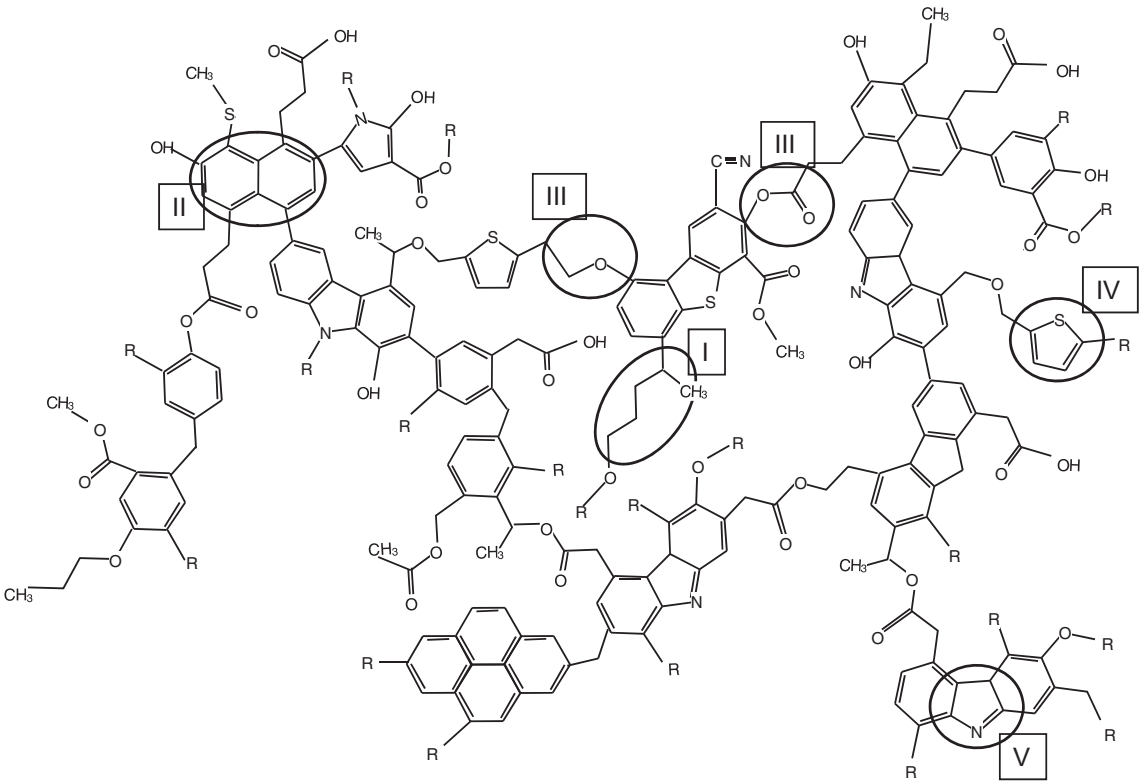

Fig. 3. Model of molecular structure of the insoluble organic matter of Murchison highlighting the region of interest discussed in the Cosmochemical Implications section. ROI **I** shows the aliphatic linkages, ROI **II** the aromatic moieties, ROI **III** the oxygenated functions, ROI **IV** the S-containing functions, and ROI **V** the N-containing ones.

chemistry, organic molecules produced in the gas phase are mainly hydrogen-poor (Herbst and Millar 2008) and can form long carbon chains. The situation is different on grains. On grains, solid CO can be hydrogenated via reactions involving atomic hydrogen and producing CH_3CO, CH_3CHO, C_2H_5OH among others (Charnley 2001). These molecules are released in the gas phase when the temperature allows the sublimation of grains, i.e., during the formation of YSOs.

Little is known about the gaseous organic fraction in the T-Tauri disks because of the observational difficulties linked to these small astronomical objects (the radius of these disks is commensurable with the present-day solar system dimensions). Most of our knowledge about this fraction comes from the study of the volatile organic molecules outgassed from comets (Bockelée-Morvan et al. 2004). They are the parent species evaporated from the icy core of the comets. A robust correlation in the relative abundances is found between these cometary species and interstellar molecules, demonstrating that the volatile fraction observed in the parent cores of T-Tauri disk is incorporated into the solar system bodies that were formed at temperatures down to 30 K.

Polycyclic Aromatic Hydrocarbons

Because their small sizes allow them to be heated to high temperatures, the polycyclic aromatic hydrocarbons (PAHs) were first proposed as the carriers of the aromatic IR bands observed in the diffuse interstellar medium (ISM). Based on the IR features of these PAHs, their carriers were attributed to a compound comprising at least hundreds of carbon atoms. Although most models conclude that astronomical PAH consist of 50 carbon atoms on average, i.e., ≈20 aromatic rings (Pendleton and Allamandola 2002; Visser et al. 2007; Tielens 2008), the size of aromatic moieties in interstellar space remains an open issue (Kwok 2004). For example, quenched carbonaceous composites were produced by heating CH_4 up to 3000 K followed by a rapid expansion into a vacuum chamber and condensation at room temperature (Sakata et al. 1987). The mass spectrometry of the resultant material suggests that most of their aromatic components have only one to two rings, i.e., 10 carbon atoms. Although it is not yet certain what material gives the best approximation for the interstellar carbonaceous dust (Kwok 2004), it is clear that it includes both aromatic and aliphatic components.

In T-Tauri disks, the IR emission feature is attributed to the presence of 100 C-atom PAHs having a 1/1 mixture of neutral and ionized molecules. The variations in the relative abundances of the PAHs are due to their photodissociation caused by the intense ultraviolet (UV) radiation field caused to the central star (Ehrenfreund et al. 2006; Visser et al. 2007). The lack of detection of these PAHs in different disks is attributed to the low efficiency of visible photons exciting PAHs but not to their absence in the disk. The organic composition of the solar T-Tauri disk is now better known from the analyses of the samples returned from The Stardust space mission (Sandford et al. 2006). In Stardust samples, many organic species are PAHs with typical size much smaller than those from the interstellar space, i.e., a few aromatic rings.

The PAHs observed in disks are not attributed to an in situ formation process after the collapse and main infall phases. They are rather considered as interstellar products. Indeed, the formation and growth of PAHs in a disk would require (1) high temperatures (approximately 1000 K), (2) high density, (3) high abundance in the aromatic ring precursors—presumably acetylene? (Frenklach and Feigelson 1989; Cherchneff and Barker 1992) and (4) for the smallest PAHs, a low UV radiation field to prevent their rapid photodissociation. However, experimental simulations have shown that (Nuth et al. 2008), at temperatures between 500 and 900 K, a carbonaceous coating is formed on grain surfaces via Fischer–Tropsch type reactions by self-perpetuating catalytic reactions. The macromolecular structures of this coating resemble those found in the presently modeled chondritic IOM, suggesting in turn that T-Tauri disks are able to produce fairly large quantities of the precursors of the IOM.

In most T-Tauri disk models, these conditions correspond to regions close to the central star (< 0.1 AU) and it is unlikely that this in situ production of PAHs affects the interstellar PAH population observed at larger radii in the disk (Visser et al. 2007). This conclusion has been reached by a detailed study of the destruction rates of PAHs by UV photons, in T-Tauri disks (Siebenmorgen and Krugel 2010).

Comparison With the ISM

The "Universal IR Spectrum" Around 3.3 μm

The structure reported in Fig. 1 yields the spectrum observed around 3.3 μm in the diffuse ISM (Galactic and extra-Galactic; Pendleton and Allamandola 2002). Such a spectrum is peculiar in the sense that the $-CH_2/-CH_3$ ratio in aliphatics is close to 2 (Ehrenfreund et al. 1991, 1992). In Murchison, this ratio measured through NMR is 2 (Gardinier et al. 2000). These values are much lower than those found in terrestrial kerogens where long chains—with $[CH_2/CH_3] > 10$—occur within the macromolecule. As highlighted as ROI **I** in Fig. 3, this ratio results from the combination of two features: aliphatic chains are short and highly branched. The low value of this ratio results from the statistical combination of C and H in short aliphatic chains exhibiting all its possible isomers. For example, a single chain of five carbons attached to a unit has a CH_2/CH_3 ratio of 4/1, whereas the same chain with five carbons exhibiting all the possible isomers has a CH_2/CH_3 ratio of 3/2. Such a tendency for the CH_2/CH_3 ratio to decrease through isomerization is a general rule. It can thus be stated that the low $-CH_2/-CH_3$ ratio of the extraterrestrial organic matter is a direct consequence of the random distribution of C and H in aliphatic chains. This distribution is a signature for the absence of biochemical activity governing the chain elongation mechanism. This statement applies to both the Solar and the Interstellar organosynthesis.

Aromatic–Aliphatic Relationship

Spectroscopic and microscopic data on IOM revealed that aromatic moieties comprise a relatively low proportion of protonated carbons thus suggesting that they are highly substituted. It can be reasonably assumed that aromatic moieties in such materials are derived from cyclization and aromatization of linear chains. As a result, the more branched the linear chains, the more substituted the aromatic rings. The high branching level in the aliphatic units is therefore fully consistent with the low level of protonation of the aromatic moieties. These specificities give a basis for a model of organic synthesis in space: the insoluble matter would result from a statistical combination of all possible bonds involving CH_3, CH_2, and CH radicals in the gas phase, producing both aliphatic and aromatic moieties. Such free organic radicals would be the result of energetic radiations such as cosmic rays or UVs. In such a model, the organic synthesis would take place by successive addition of single-carbon units as previously suggested by Herbst (2001) through two potential mechanisms (insertion of carbon or radiative association). Such an elongation process would end by a spontaneous cyclization when the chain length exceeds about seven carbons. This process can be illustrated by the following schematic reaction:

$$CH_i + C_nH_j \rightarrow C_{n+1}H_{i+j}.$$

When the principal chain of the aliphatic radical has more than seven carbons, the cyclization spontaneously takes place followed by aromatization. This cyclization is made especially possible in the gas phase. Such a

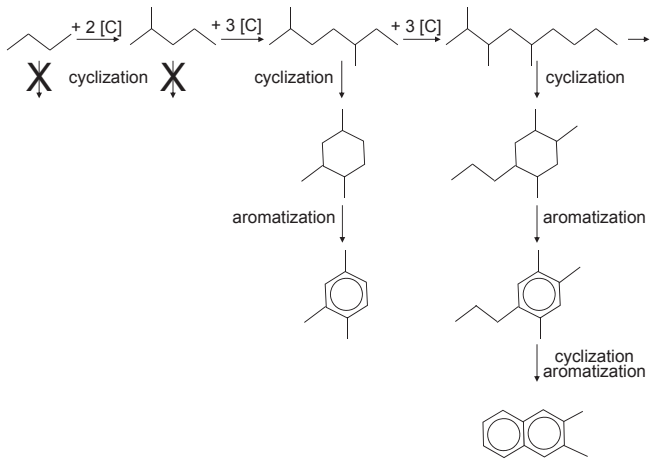

Fig. 4. Illustration of a possible formation pathway of aromatic moieties in the gas phase. The starting drawing accounts for an ion or radical with four carbon atoms. H atoms are not indicated for the sake of clarity. Such a scheme does not take into account heteroelements.

cyclization/aromatization process is commonly observed, for example, upon thermal treatment of aliphatic polymers (Madorsky 1964). Fused rings are then formed through the classical mechanism of annealing. A schematic example is given in Fig. 4. As a result, (1) no long linear chains contribute to the macromolecular network and (2) aromatics are highly substituted because of the highly branched nature of the aliphatics.

Another mechanism might be a priori considered: it involves the addition of aliphatic chains onto pre-existing aromatic moieties. This would be favored by the presence of aromatic radicals which would capture aliphatic radicals. A recent observation tends to rule out this mechanism. NanoSIMS examination of Murchison shows that the organic matter that exhibits high D enrichments (interpreted as related to organic free radicals) is heterogeneously distributed both in bulk IOM and in bulk rock (Rémusat et al. 2009). In other terms, organic radicals seem not to be the nucleus of the polymerization of the whole IOM.

Unfortunately, because of the present lack of experimental simulation, it is not possible to specify (1) the nature of the reactants (ions, radicals, and neutral species), (2) an involvement of a possible catalyst in the condensation reactions (grain surfaces?), and (3) the physicochemical conditions (T, redox, etc.) that prevailed at the time of the IOM formation. Because of its high D/H ratio, this IOM was often regarded in the literature as formed at low temperature ($T < 200$ K) (Robert 2006). However, for the Orgueil meteorite, it has been shown recently that the Deuterium was added to the IOM after its formation (Remusat et al., 2006). Therefore, the temperature at which the above mechanism can take place can be as high as 650 K, i.e., the temperature above which the aliphatic chains start to become unstable.

Note that the rings are far from being saturated in H. If the chain elongation involves ion chemistry, the neutralization process produces fragments that tend to have at least one H atom less than the parent ion; this is illustrated by the following dissociation recombination reaction: $C_nH_2^+ + e \rightarrow C_nH + H$ (Herbst and van Dishoeck 2009). As in the T-Tauri disk half of PAHs are ionized (Tielens 2008), the fact that rings are unsaturated in the IOM reinforces the idea that the matter present in meteorites was condensed in a highly ionized medium.

The Size of the Aromatic Units

The aromatic (ROI **II** in Fig. 3) units that occur in the macromolecular structure of the IOM are clearly much smaller than those postulated for interstellar PAHs (Allamandola et al. 1999; Galvez et al. 2002; Kwok 2004). The size of interstellar PAHs has been extensively discussed in the astronomical literature to account for the features of the IR spectra as well as in the models of their formation, evolution, and destruction (see, for example, the reviews by Tielens 2008 and Herbst and van Dishoeck 2009). Akin to the molecular model proposed here for the chondritic IOM, several two-dimensional molecular models have been published for interstellar PAHs. They all involved moieties having C_{50}–C_{100} in size. A similar situation exists when comparing the PAHs from the comet Wild 2 analyzed in the samples returned to Earth by The Stardust mission: PAHs in Wild 2 are also much smaller than their interstellar counterpart. Such dissimilarity must be considered as a serious problem as far as the origin of the organic matter in the solar system is concerned.

There are two ways out of this problem:

1. The chondritic IOM results from the fragmentation of larger interstellar PAHs by photodissociation (Derenne et al. 2005). Based on the recent observations made by the Spitzer Space Observatory, a reappraisal of this interpretation was made by several authors (Geers et al. 2006; Visser et al. 2007; Siebenmorgen and Krugel 2010). They have shown that virtually all PAHs must be destroyed at disk distances where the telluric planets and the parent body meteorites formed. As PAHs are nevertheless observed in T-Tauri disks and as the formation of PAHs in the opaque zones of the disks—i.e., inaccessible to optical observation—is supposed to be too slow to compete with their destruction, they suggest that the turbulent vertical replenishes the surface of the disk.

2. The chondritic IOM is formed in the hottest part of the solar T-Tauri disk (Nuth et al. 2008) and redistributed over large distances by turbulence (Bockelée-Morvan et al. 2002).

Although the first interpretation cannot be dismissed, the second one seems more in accordance with the isotopic compositions of the IOM.

Parent Body Alteration Signatures

It must be emphasized here that as the D/H ratio is higher in organics than in clays, an organosynthesis taking place in circulating fluids of the parent body can be ruled out. Consequently, this organic matter has been synthesized in another environment than the parent body and then has been mixed with the precursors of the mineral matrix. However, once in the rock, the circulation of the water may have altered the molecular structure and the chemical/isotopic compositions. This process of alteration is discussed in this section.

Oxygen and Sulfur Speciation

The molecular speciation of oxygen and sulfur in chains can be regarded as the consequence of the alteration of the parent body. The main evidence for such a conclusion was derived from the comparison between the Murchison and the Orgueil meteorites.

The oxygen-containing functions are probably related to the aqueous alteration experienced by primitive carbonaceous chondrites. Indeed, warm water circulation could have resulted in an oxidation of IOM leading to the formation of ether or ester functional groups. Upon pyrolysis (Remusat et al. 2005b), a higher amount of phenols and substituted homologs are released from Orgueil than from Murchison in agreement with the higher oxygen content obtained from the elemental analyses of Orgueil (16.6 wt%) compared with Murchison (14.5 wt%). In addition, the pyrolysis and ruthenium tetroxide oxidation results suggest that in Orgueil, oxygen is preferentially connected to aromatic carbons as in phenols, whereas in Murchison, oxygen is more often located within the aliphatic linkages as ester or ether functional groups as shown by ROI **III** in Fig. 3.

When Orgueil and Murchison are compared, a much higher content of total sulfur is noted in Murchison according to elemental analysis. X-ray diffraction and K-edge sulfur XANES revealed that 29% of the sulfur in Murchison occurs as minerals (17% of sulfide such as pentlandite and 12% of sulfate), whereas all sulfur was considered to be organic in Orgueil. However, the resulting organic sulfur is still three times more abundant (with respect to carbon) in Murchison than in Orgueil. In addition to this major quantitative difference, the nature of the organic sulfur also differs between the two meteorites. If in both cases, the organic sulfur mainly occurs as aliphatic sulfides and thiophenes (see ROI **IV** in Fig. 3), the sulfides to thiophenes ratio is 1.3 in Orgueil and 3.1 in Murchison (Derenne et al. 2002; Remusat et al. 2005b). This higher relative contribution of thiophenes with respect to aliphatic sulfides in Orgueil points to a higher hydrothermal event in this meteorite, as it is known that aliphatic sulfides are converted into thiophenes under thermal stress (Riboulleau et al. 2000).

Relationship Between Soluble and Insoluble Organic Fractions

Thanks to solid-state ^{15}N NMR, it was shown that nitrogen is mainly contained within pyrrole functions (see ROI **V** in Fig. 3). The virtual lack of amide groups in the IOM a priori prevents this macromolecule from being the source of the amino acids that occur in the soluble fraction of the carbonaceous chondrites. Moreover, as discussed in Remusat et al. (2005b), the comparison of the D/H, $^{15}N/^{14}N$ and $^{13}C/^{12}C$ isotopic ratios points also against a common origin for IOM and soluble amino acids. Conversely, amino acids would therefore be derived from another reservoir of nitrogen. For instance, UV irradiation of HCN-rich interstellar ices (in the presence of aldehydes and/or ketones) can yield amino acids (Lerner 1997; Muñoz Caro et al. 2002). 9

By contrast, other moieties of the IOM are supposed to share a common origin with their soluble counterparts. They comprise the aromatic hydrocarbons as reported by Pering and Ponnamperuma (1971). Moreover, Huang et al. (2007) have shown that the soluble aliphatic acids are related to the aliphatic linkages of the IOM (based on their $^{13}C/^{12}C$ and D/H ratios).

Therefore, the soluble fraction seems to be a mixture of products derived from different processes—hydrothermal degradation of the IOM, reactions in ice mediated by UV light, terrestrial contamination, etc. This is at variance with what is commonly expected, i.e., a continuum from small soluble molecules to large insoluble ones. Another explanation might be that soluble compounds are derived from a precursor which has now be totally converted into the products, the IOM being the leftover part of an initially more composite material.

IOM Features Reveal an Organosynthesis in the Solar T-TAURI Disk?

As pointed out by Alexander et al. (2007) and experimentally shown by Nuth et al. (2008), efficient

synthesis of PAHs from simple linear hydrocarbons in solar gas requires high temperatures (1100–900 K) and pressures (10^{-7}–10^{-6} bars). Alexander et al. (2007) therefore estimated that the IOM production is unlikely to take place in the solar nebula. However, several features of the IOM chemical structure point to a formation in the Solar T-Tauri disk as discussed below. As already mentioned above, our interpretation of the small size of the aromatic moieties is one of them. Additional indices are provided by the nature of the free radicals (as studied using EPR), D/H distribution at the molecular level and the location of noble gases in the so-called organic-rich Q-phase. These points are successively addressed below.

Electron paramagnetic resonance revealed the presence of a significant amount of organic free radicals in the IOM from Murchison. These free radicals are organized as clusters with high local concentrations compared to the bulk IOM (Binet et al. 2002). Such a heterogeneity seems to be unique among the natural organic macromolecules and therefore can be regarded as a specificity for extraterrestrial organic matter (in addition to Orgueil and Murchison, it was also observed in Tagish Lake, Binet et al. 2004a). Moreover, it must be noted that as in terrestrial samples, these free radicals survive the drastic acid treatments used to isolate the IOM (Binet et al. 2002).

Moreover, diradicaloid structures were found in the same IOMs (Binet et al. 2004a, 2004b). Such structures are highly reactive thus suggesting that they are protected within microdomains. The formation mechanism of these radicals is still unknown but based on their chemical structure, one can assume that they indicate two possible origins: (1) a condensation of small aromatic moieties in a highly irradiated medium (UVs, cosmic rays, and stellar winds) and (2) a quench condensation of hot aromatic radicals in a cold gas, thus preventing the pending bonds to capture H·. Interestingly, these two environments can be reproduced in the laboratory. Preliminary experiments point to the formation of diradicaloids during the quench condensation of rings from a gas phase. However, their organization in clusters remains puzzling. Because the physicochemical conditions of their synthesis are, at the present time, largely unknown, producing these diradicaloids in laboratory experiments represents a challenge that would yield new constraints on the conditions of the formation of the IOM. Anyhow, their formation during the hydrothermal event appears highly unlikely as water tends to erase the radicals.

Two additional observations are also in favor of an organosynthesis in the T-Tauri disk, although they were so far only reported in Orgueil IOM.

Recent studies combining NanoSIMS and pulsed EPR data have demonstrated that the organic radicals are the carriers of an exceptional deuterium enrichment (Gourier et al. 2007), probably acquired after the formation of the macromolecular network. Such a secondary deuteration process is difficult to reconcile with the low density of the interstellar medium. At the present time, the simplest explanation is to admit that this isotope exchange had taken place in the UV-irradiated regions of the T-Tauri Solar disk.

Xenon and likely the other noble gases, which are mass dependently fractionated relative to the solar composition, are mechanically trapped (i.e., not adsorbed or embedded inside the carbon rings) between the lattices of the macromolecular layers of the IOM (Marrocchi et al. 2005). Such a location is also difficult to reconcile with a direct condensation in the ISM where the low xenon density prevents such an addition by simple trapping ([H] < 10^3 cm^{-3} corresponding to [Xe] < 10^{-13} cm^{-3}).

Acknowledgment—Pascale Ehrenfreund is warmly thanked for helpful comments on a previous version of the manuscript.

Editorial Handling—Dr. A. J. Timothy Jull

REFERENCES

Alexander C. M. O'D., Fogel M., Yabuta H., and Cody G. D. 2007. The origin and evolution of chondrites recorded in the elemental and isotopic compositions of their macromolecular organic matter. *Geochimica et Cosmochimica Acta*.

Allamandola L. J., Hudgins D. M., and Sandford S. A. 1999. Modeling the unidentified infrared emission with combinations of polycyclic aromatic hydrocarbons. *The Astrophysical Journal* 511:L115–L119.

Behar F. and Vandenbroucke M. 1986. Représentation chimique de la structure des kérogènes et asphaltènes en fonction de leur origine et de leur degré d'évolution. *Revue de l'Institut Français du Pétrole* 41:173–188.

Binet L., Gourier D., Derenne S., and Robert F. 2002. Heterogeneous distribution of paramagnetic radicals in insoluble organic matter from the Orgueil and Murchison meteorites. *Geochimica et Cosmochimica Acta* 66:4177–4186.

Binet L., Gourier D., Derenne S., Pizzarello S., and Becker L. 2004a. Diradicaloids in the insoluble organic matter from the Tagish Lake meteorite: Comparison with the Orgueil and Murchison meteorites. *Meteoritics & Planetary Science* 39:1649–1654.

Binet L., Gourier D., Derenne S., Robert F., and Ciofini I. 2004b. Occurrence of abundant diradicaloid moieties in the insoluble organic matter from the Orgueil and Murchison meteorites: A fingerprint of its extraterrestrial origin? *Geochimica et Cosmochimica Acta* 68:881–896.

Bitz M. C. Sr. and Nagy B. 1966. Ozonolysis of "polymer-type" material in coal, kerogen, and in the Orgueil

Earth and Planetary Science Letters 272 (2008) 476–480

Contents lists available at ScienceDirect

Earth and Planetary Science Letters

journal homepage: www.elsevier.com/locate/epsl

Molecular evidence for life in the 3.5 billion year old Warrawoona chert

Sylvie Derenne [a,*], François Robert [b], Audrey Skrzypczak-Bonduelle [a,c], Didier Gourier [c], Laurent Binet [c], Jean-Noël Rouzaud [d]

[a] UMR CNRS 7618 BioEMCo, 11 rue P. M. Curie, 75231 Paris cedex 05, France
[b] LEME, UMS CNRS 62, MNHN, 61 rue Buffon, 75005 Paris, France
[c] LCAES, UMR CNRS 7574, ENSCP, 11 rue P. M. Curie, 75231 Paris cedex 05, France
[d] Laboratoire de Géologie, UMR CNRS 8538, ENS, 24 rue Lhomond, 75231 Paris cedex 05, France

ARTICLE INFO

Article history:
Received 10 July 2007
Received in revised form 26 March 2008
Accepted 13 May 2008
Available online 23 May 2008

Editor: C.P. Jaupart

Keywords:
chert
kerogen
Precambrian
biomarker
early life

ABSTRACT

The biological origin of organic matter in the oldest siliceous sediments (cherts) is still debated. To address this issue, the insoluble organic matter (kerogen) was isolated from a chert of the Warrawoona group. The chemical structure of the kerogen was investigated through a combination of analytical techniques including solid-state ^{13}C nuclear magnetic resonance and pyrolysis. Although dominated by aromatic hydrocarbons, the pyrolysate comprises a homologous series of long chain aliphatic hydrocarbons characterized by odd-over-even carbon number predominance. This distribution is only consistent with a biological origin. As kerogen must be contemporaneous of the solidification of the chert, this observation should be regarded as an evidence for the presence of life on Earth, 3.5 By ago.

1. Introduction

Cherts are amongst the oldest sedimentary rocks on Earth and offer a remarkable record of well-preserved microfossils throughout the Precambrian. Based on spectroscopic and morphological observations, microstructures in the 3.5 By old Apex chert from the Warrawoona group in Australia have been attributed to fossil cyanobacteria and thus would constitute the oldest evidence for life on Earth (Schopf, 1993). In addition to morphological criteria, the carbonaceous nature of the microstructures established by Laser Raman microspectroscopy was considered as an evidence for their biogenicity (Schopf et al., 2002). However, the validity of this criterion as evidence for life has been questioned and it is now accepted that Raman spectroscopy alone cannot assess biogenicity (Pasteris and Wopenka, 2002). Moreover, it was shown that abiotic synthesis (Fischer–Tropsch) is able to yield organic microstructures exhibiting similar morphological features and Raman spectra as the putative microfossils from the Apex chert (Brasier et al., 2002; Garcia-Ruiz et al., 2003). Carbon isotope composition was also often put forward as an additional criterion of the biological origin of the organic matter in the Archean cherts (Mojzsis et al., 1996; Schidlowski, 2001). However, once again, this approach was shown not to be univocal, as abiotic processes can lead to similar fractionation (Horita and Berndt, 1999; Van Zuilen et al., 2002; McCollom and Seewald, 2006). More recently, the wide diversity in the morphological features of the stromatolites from Strelley Pool chert and the continuity in the carbonaceous matter record in rocks >3.0 By suggested that most OM in these rocks was produced by living organisms (Allwood et al., 2006; Tice and Lowe, 2006).

A new criterion, in the form of an indisputable biomarker, is therefore needed in order to resolve the debate about when life first appeared on Earth. Biomarkers characteristic of cyanobacteria were reported in the soluble organic fraction of the ca. 2.7 By old shales from Hamersley Basin in Australia (Brocks et al., 1999). However, evidence drawn from soluble organic matter is disputable because there are several potential sources of post-depositional contamination, notably subsurface biological activity and groundwater penetration. Although such issues have been carefully evaluated in the case of Hamersley Basin shales (Brocks et al., 1999), the synchronism between the formation of soluble molecular fossils and the host rock remains difficult to demonstrate (Brocks et al., 2003a; Brocks et al., 2003b). In contrast, it is generally accepted that the insoluble macromolecular organic matter characterized by covalent bonds is syngenetic with the host rock hence an increasing interest for this organic fraction (Brocks et al., 2003a; Marshall et al., 2006; Marshall et al., 2007). We have therefore isolated the kerogen from a chert of the lowest metamorphic grade from the Warrawoona Group and investigated its chemical structure using a combination of spectroscopic and pyrolytic tools.

* Corresponding author. Tel.: +33 144 27 67 16.
E-mail address: sylvie-derenne@enscp.fr (S. Derenne).

0012-821X/$ – see front matter © 2008 Elsevier B.V. All rights reserved.
doi:10.1016/j.epsl.2008.05.014

2. Methods

The sample (PPRG 006 from Precambrian Palaeobiology Research Group collection, courtesy of W. Schopf) was selected for this study from a large collection of cherts on the basis of its isotopic composition (see below). It was collected in the lower chert horizon of the Towers Formation in the North Pole B Deposit Mine from the upper lip of the open cut on the west side; Marble Bar 1:250,000 map sheet grid ref n°. 223357 (Walter et al., 1983). The North Pole Dome, from which the sample was collected, is situated 30 km NW of the Apex cherts in the Marble Bar region. Since 1983, the Towers Formation cherts at The North Pole Mine have been reassigned to the Dresser Formation, which has an age of ca. 3.490 By (van Kranendonk, 2006).

The insoluble organic matter was isolated from the ground chert as follows: stirring at room temperature for several hours in dichloromethane/methanol, 2/1, v/v in order to remove soluble organics, followed by demineralization using the classical HF/HCl treatment (Durand and Nicaise, 1980) and further solvent extraction. After each treatment, the insoluble residue was recovered by centrifugation.

Variable amplitude cross-polarization/magic angle spinning (VACP/MAS) solid-state ^{13}C nuclear magnetic resonance (NMR) spectrum was obtained at 100.62 MHz for carbon (Bruker Avance 400 spectrometer, recycle time 5 s, contact time 1 ms), using a high spinning rate (20 kHz) to spin out chemical anisotropy and avoid spectrum disturbance by spinning side bands.

Curie point pyrolysis-gas chromatography/mass spectrometry (CuPy-GC/MS) was performed with a Fischer 0316 flash pyrolyser. The sample (ca. 2 mg) was pyrolysed for 10 s using ferromagnetic tubes with a Curie temperature of 650 °C under a 5 ml min^{-1} He flow. The pyrolyser was directly coupled to the GC/MS: a HP-5890 gas chromatograph (30 m CPSil5CB capillary column, i.d. 0.25 mm, film thickness 0.5 μm) and a HP-5889A mass spectrometer (electron energy 70 eV, ion source temperature 205 °C, scanning from 40 to 650 a.m.u, 0.7 scan/s). The GC oven was programmed from 100 to 300 °C at a rate of 2 °C min^{-1} after a first stage at 100 °C for 10 min.

High resolution transmission electron microscopy (HRTEM) observations were carried out using a Jeol 2011 microscope operating at 200 keV. Image analysis was conducted after skeletonization as described by Rouzaud and Clinard (2002).

3. Results and discussion

Demineralization of 149.5 g of crude rock yielded 32.7 mg of kerogen, i. e. 218 ppm. The carbon content (53.4%) of the isolated kerogen indicates that most of the initial carbon of the rock is recovered in this insoluble fraction, since the crude rock contains 121 ppm of carbon (Beaumont and Robert, 1999). The elemental composition gives an atomic H/C ratio of 0.62, indicating a rather aromatic character. This kerogen concentrate also contains mineral phases, such as titanium and chromium oxides, as revealed by SEM-EDS. These oxides, which are known to survive HF / HCl treatment, were previously observed by Kato and Nakamura (2003) on crude cherts from Warrawoona.

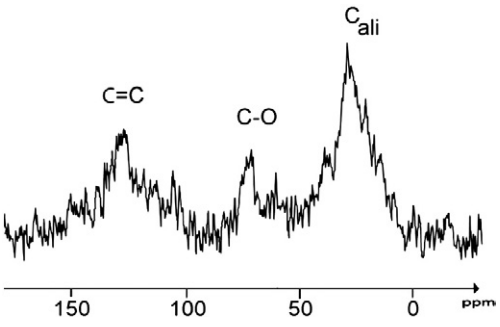

Fig. 1. Solid state variable amplitude CP-MAS ^{13}C NMR spectrum of the kerogen from the Warrawoona chert.

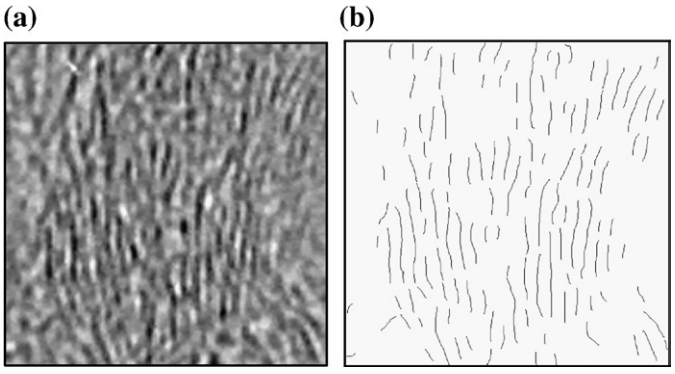

Fig. 2. HRTEM image (10×10 nm) of the kerogen from the Warrawoona chert and corresponding skeletonized image.

The solid-state ^{13}C cross-polarization/magic angle spinning nuclear magnetic resonance (CP/MAS NMR) spectrum of the isolated kerogen (Fig. 1) is dominated by a broad signal centered at 29 ppm due to aliphatic carbon atoms and shows two relatively minor peaks at 70 and 130 ppm, assigned to C–O and unsaturated carbons, respectively. Although solid-state CP/MAS ^{13}C NMR is known to overestimate aliphatic carbons, it must be noted that the presence of alkyl chains is also observed through Fourier transform Infrared (FTIR) spectroscopy (not shown). Indeed, the spectrum of the Warrawoona chert exhibits the typical bands for CH_2 and CH_3 in the 2850–2965 cm^{-1} range. The 2925 cm^{-1} and 2850 cm^{-1} bands are due to asymmetrical and symmetrical stretching vibrations of CH_2 groups. The asymmetrical stretching band of the CH_3 groups can be clearly seen at 2965 cm^{-1}. A band at 1585 cm^{-1} reflects the stretching vibration of aromatic C=C whereas carbonyl functions are detected at 1710 cm^{-1}. The broad band around 1160 cm^{-1} may be due either to ether functions or to residual silica. The NMR spectrum strongly differs from those of mature kerogens, for which the 30 ppm peak is virtually absent due to thermal release of alkyl chains upon maturation (Miknis et al., 1982). As a result, the NMR spectrum of the Warrawoona chert indicates that this material, although 3.5 By old, did not experience any severe, thermally induced chemical modification.

This may appear at variance with the Archean age of the sample. However, the Warrawoona Group has been described as the one which underwent the lowest metamorphism and which contains the best preserved Archean stratigraphic succession on Earth (Van Kranendonk et al., 2002). Moreover, the carbonaceous matter structure, which cannot be used to determine the biological origin (or not) of the sample, can provide powerful information about its thermal history as recently stressed by Tice and Lowe (2006). Indeed, large “graphitic domains” are commonly reported when the sample reached the metamorphic grade of prehnite–pumpellyite (Wedeking and Hayes, 1983). In contrast, our observations of the PPRG 006 sample through high resolution transmission electron microscopy (HRTEM) (Fig. 2) and further image analysis showed relatively large aromatic units but no such “graphitic domains” (PPRG 006 exhibits a mean layer extent about 1.1 nm, corresponding to about 15 fused aromatic rings (Rouzaud et al., 2005)). It must be noted that the occurrence of these large aromatic units is not at variance with the presence of aliphatic carbons in the FTIR and NMR spectra as the latter cannot be detected through HRTEM. However the organization degree is far from having reached the graphite crystalline stage. Indeed, the interlayer spacing is 0.39 nm, significantly higher than the graphite value (0.3354 nm). These observations are in perfect agreement with a recent study of the Apex chert through TEM and electron energy loss spectroscopy (EELS) (de Gregorio and Sharp, 2006). Taken

together, these data point to a rather low metamorphic grade for the Warrawoona sample in agreement with previous reports.

This was confirmed by Curie point pyrolysis-gas chromatography coupled with mass spectrometry, which we performed on the same sample using ferromagnetic wires with a Curie temperature of 650 °C. As shown in Fig. 3a, the trace of the pyrolysate is dominated by a wide range of aromatic compounds along with a series of *n*-alkane/*n*-alk-1-ene doublets up to C_{25}. The aromatic compounds comprise hydrocarbons (PAHs) along with thiophenic and phenolic products. PAHs are dominated by toluene, styrene, naphthalene, methylnaphthalenes and fluorene. Significant contributions of indene and anthracene/phenanthrene derivatives are also noted in the pyrolysate. The largest PAHs detected under our analytical conditions is fluoranthene. This rather large production of PAHs upon pyrolysis is expected due to the aromatic character of the sample as revealed by spectroscopic analyses and HRTEM. Thiophenic compounds include C_1 to C_4-thiophene, C_1 to C_2-benzothiophene and C_0 to C_1-dibenzothiophene. C_0 to C_3-phenol are also identified in the pyrochromatogram. These phenols are distinct from those commonly observed in pyrolysates of lignin-derived material. They are likely formed through the cleavage of aromatic ether bonds, as observed in meteorite pyrolysates (Remusat et al., 2005b).

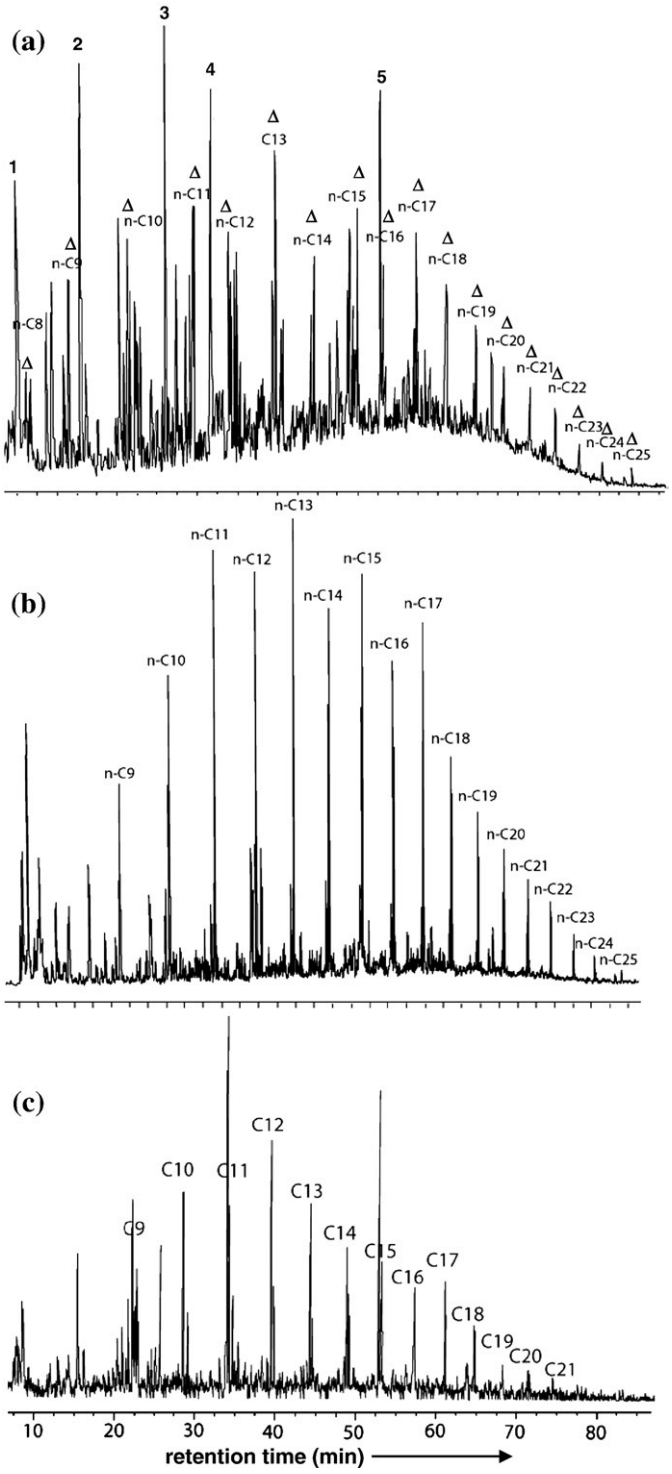

Fig. 3. Curie point pyrolysis at 650 °C: a) Total ion current trace of the pyrolysate. Δ refers to the *n*-alkane/*n*-alkene doublets, 1: toluene, 2: styrene, 3: methylphenol, 4: dimethylphenol, 5: fluorene b) Ion chromatogram at m/z 57 showing the distribution of the *n*-alkanes. c) Ion chromatogram at m/z 58 showing the distribution of the *n*-alkanones.

In addition to these, dominant, aromatic products, several series of aliphatic compounds contribute to the pyrolysate. A series of *n*-alkane/*n*-alk-1-ene doublets up to C_{25} is thus identified (Fig. 3b). These alkanes and alkenes originate from the homolytic cleavage of long alkyl chains through capture and elimination of H° radicals, respectively. A series of *n*-alkylbenzenes up to C_{22} can also be identified in the pyrolysate along with its higher homologue (*n*-alkyl, methylbenzenes). These products result from the cyclization of the alkyl radical, thus confirming the presence of long chains covalently linked to the macromolecular network. An additional series of aliphatic compounds, namely *n*-alkan-2-ones, was identified in the pyrolysate of the Warrawoona chert. Its distribution (from C_9 to C_{21}) is shown by the ion chromatogram at m/z 58 (Fig. 3c). Such ketones are formed upon pyrolysis through homolytic cleavage of ether bonds. Their presence in the pyrolysate is therefore consistent with that of C–O groups inferred from spectroscopic data. The formation of such ether bonds through oxidative cross-linking was shown to be favoured by silicification in a 93 million years-old chert from Italy although such linkages also occur in the organic matter from non-cherty rocks (Salmon et al., 2003). Therefore the oxidative formation pathway of the kerogen seems to be mediated by silicification, pointing to syngeneity between the cherty matrix and the kerogen.

Under laboratory conditions, C–C bonds in alkyl chains are known to be cleaved at 400 °C (within a few tens of minutes) and can be cleaved at lower temperatures on longer time scales. As a result, the release of the alkane/alkene doublets upon pyrolysis confirms that the kerogen of Warrawoona was never exposed to high temperatures for any significant time period.

The pyrochromatogram of the Warrawoona chert at 650 °C shows a slight predominance of odd carbon numbered *n*-alkane/*n*-alk-1-ene doublets (Fig. 3a). It must be noted that the alkylbenzenes, which also originate from alkyl chains, exhibit a similar predominance in the same carbon number range. The distribution of the *n*-alkanes in the pyrolysate can be described more accurately by using the ion chromatogram at a mass-to-charge ratio (m/z) of 57 (Fig. 3b). It must be noted that no classical biomarker of recent organic matter such as pristane, phytane, sterane or hopane could be detected in the pyrolysate in spite of a careful search using their characteristic mass fragments. More generally, a virtual lack of branched alkanes is noted. Taken together, the lack of branched compounds and the slight odd-over-even carbon number predominance make the distribution of the alkanes from the Warrawoona chert pyrolysate strongly different from that obtained from organic matter formed abiotically under any known natural or laboratory conditions. Indeed, upon pyrolysis under the same experimental conditions as described above, the abiotic macromolecular organic matter from carbonaceous chondrites yields a virtual lack of aliphatic products (Remusat et al., 2005b; Sephton et al., 2004). Moreover, these abiotic extraterrestrial aliphatic compounds exhibit the maximal diversity of isomers, i.e. all the branched isomers are present for any given carbon number. A similar diversity of isomers in abiotic insoluble organic macromolecules from carbonaceous chondrites is also observed when the aliphatic linkages

were exposed to RuO_4 oxidation, attesting there is no bias induced by this pyrolysis (Remusat et al., 2005a). Moreover, a similar diversity of isomers was observed in the soluble hydrocarbons formed upon thermal decomposition of siderite, i. e. resulting from an abiotic process (McCollom, 2003). It was recently stressed that thermo-catalytic reactions yield homologous series of organic compounds with no carbon number preferences (Rushdi and Simoneit, 2001) and that Fischer–Tropsch-type products are dominated by unbranched alkanes with a characteristic linear decrease in abundance (McCollom and Seewald, 2006). In contrast, a weak odd-over-even carbon number predominance is a unique characteristics of organics formed biologically since it reflects biosynthesis using addition of C2 units (Albro, 1976). The C_{10}–C_{18} range in the alkanes of the Warrawoona pyrolysate is characterized by such odd-over-even carbon number predominance (Fig. 3b), confirming the involvement of a biosynthetic pathway in the formation of these *n*-alkyl chains (a carbon preference index value of 1.2 is calculated in this range (Bray and Evans, 1961)). As a result, Fig. 3b provides evidence for the presence of molecular markers of life in this Warrawoona sample. It must be noted that the carbon range containing the predominance (C_{10}–C_{18}) is markedly shorter than those commonly observed in Phanerozoic samples (longer than C_{25}) and, as far as we are aware, has never been reported.

As already stressed above, molecular structures that are covalently linked to a kerogen-matrix embedded in a host rock are considered to have formed contemporaneously with the host rock (Brocks et al., 2003a; Marshall et al., 2006). It is therefore crucial to establish that the hydrocarbons released from the Warrawoona chert upon pyrolysis were linked to the kerogen-matrix by such covalent bonds. Indeed, it is a common problem with geological samples that soluble organic compounds, such as hydrocarbons, can be physically trapped in the mineral matrix which prevent them from efficient solvent extraction. These labile compounds would be released upon pyrolysis, but may not have formed contemporaneously with the host rock, as discussed above. Such thermal desorption of soluble organics appears very unlikely for the Warrawoona chert because it would not have yielded *n*-alkane/*n*-alk-1-ene doublets. Indeed, the latter result from the homolytic cleavage of a covalent bond whereas only free alkanes, i.e. without co-occurrence of the corresponding *n*-alk-1-enes, are released upon thermodesorption. Moreover, so as to test whether *n*-alkanes with the characteristic odd-over-even carbon number predominance would be tightly trapped within the macromolecular network, we conducted a pyrolysis at 350 °C. This rather low temperature is commonly used to induce thermal desorption of products that were not released upon bitumen extraction (Brocks et al., 2003a). Thermal cracking of C–C bond does not take place at this low temperature and moieties covalently linked to the kerogen are not released. At 350 °C we did observe the release of thermally desorbed *n*-alkanes from the Warrawoona chert, but only in trace amounts and with a distinctly different distribution (C_{12}–C_{20}, maximum at C_{16} with no odd-over-even carbon number predominance, Fig. 4) from that reported above for the 650 °C pyrolysate. These labile alkanes therefore do not account for the typical biological distribution observed in the 650 °C pyrolysate and the aliphatic chains are thus covalently linked to the macromolecular network.

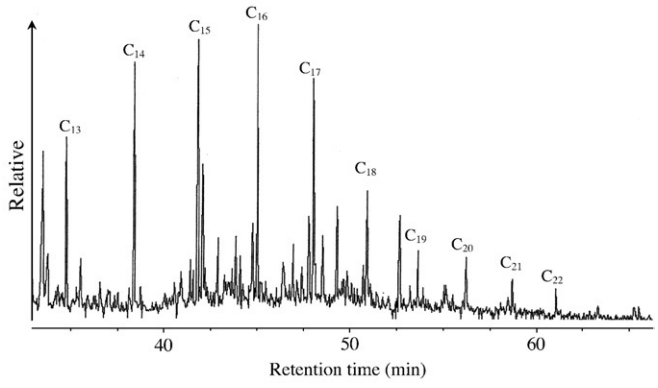

Fig. 4. Curie point pyrolysis at 350 °C: total ion current trace of the pyrolysate showing the release of *n*-alkanes.

Although it is widely accepted that kerogen has formed at the same time as the host rock, the issue of the possible laboratory or geological contamination is now addressed in greater details. Three potential types of contamination will be successively discussed: laboratory, phanerozoic and exogenous brought by the veins.

Laboratory contamination can be firmly ruled out as (i) the generated profile for the hydrocarbons is not the one typically observed for contamination (oil contamination usually results in an unresolved mixture in a lower carbon range), (ii) it should have been released through thermal desorption, (iii) the series of *n*-alkane/*n*-alk-1-ene doublets were never observed upon pyrolysis of other samples or blanks.

Phanerozoic contamination can also be excluded because (i) the commonly observed odd-over-even carbon number predominance in Phanerozoic samples appears in a distinctly higher chain length range, i. e. C_{27}–C_{31} corresponding to that of the higher plant waxes, (ii) the lack of isoprenoid hydrocarbons (pristane, phytane) in the present pyrolysate, (iii) the carbon isotope composition ($\delta^{13}C = -32.7‰$) is consistent with – although not characteristic of – a Precambrian age (Beaumont and Robert, 1999), (iv) the nitrogen isotope composition, ($\delta^{15}N = -4.1‰$, is consistent with an Archean age (Beaumont and Robert, 1999). In case of at least a partial contamination with phanerozoic organic matter, this value would have been raised up to positive values. This is especially true as nitrogen contents are higher in organic matter from young rocks than from Archean ones (Beaumont and Robert, 1999).

An *exogenous* contamination by hydrocarbons brought by the millimetre-sized veins observed within the matrix of microcrystalline quartz also seems unlikely. Indeed, these veins consist of sub-millimeter crystals of quartz and account for 7% of the bulk sample (assessed from image analysis of thin section). The oxygen isotopic composition ($\delta^{18}O$) has been analyzed by ion microprobe spectroscopy (IMS) (Robert and Chaussidon, 2006) and similar values have been obtained for both the matrix and the veins, +16.7 and +17.0‰, respectively. A different $\delta^{18}O$ signature would have been left in the veins after a late input of silica from a distinct geological formation during a metamorphic event, and here, this is not the case. Moreover, the carbon concentrations in both veins and matrix have also been determined by IMS and they show that carbon in veins only account for 3.7% of the total carbon of the whole rock. Such a low contribution rules out that the veins are the only carrier of the aliphatic chains exhibiting the biological signature.

Our data thus report the occurrence of biological markers in the kerogen embedded in a 3.5 By old chert. The nature of the biological activity must also be examined. As stressed above, the pyrolysate of the Warrawoona chert contains thiophenes. The release of organo-sulphur products upon kerogen pyrolysis is commonly considered as evidence for the involvement of the so-called sulphurisation process, which is a well-established mechanism of kerogen formation (Sinninghe Damsté et al., 1989). It involves the introduction of sulphur into potentially labile lipids and/or carbohydrates. Such intra- and intermolecular sulphur incorporations give rise to sulphur-rich macromolecules. The occurrence of such organo-sulphur moieties in the macromolecular network is consistent with scanning electron microscopy observations coupled with energy dispersive spectroscopy (EDS), which systematically have revealed the co-occurrence of sulphur and carbon in the kerogen. The incorporated sulphur originates from H_2S produced by sulphate-reducing bacteria. The presence of thiophene-containing products in the pyrolysate of the Warrawoona chert may thus point to the involvement of sulphate-

bacteria in the preservation of its organic matter. It must be noted that this hypothesis is supported by a recent study that considered microbial sulphate reduction in the 3.5 By old North Pole deposit (Shen and Buick, 2004), based on sulfur isotope measurements although it has been debated even more recently (Philippot et al., 2007). Considering non-organic sulphur, no elemental sulphur could be detected in the kerogen concentrate but barium sulphate was identified. It cannot therefore be excluded that organo-sulphur compounds would be formed upon pyrolysis through a thermo-sulphate reduction process.

Our data report the occurrence of biological markers in the kerogen embedded in a 3.5 By old chert. Several features point to a contemporaneous formation of this kerogen and its siliceous host rock. This observation supports a scenario according to which life was present on Earth 3.5 By ago.

Acknowledgements

We thank J. Maquet for technical assistance in NMR and J. Templier for pyrolysis experiments. W. Schopf is deeply acknowledged for providing the chert sample and unlimited access to relevant information. This work was supported by grants from the « Exobiologie » group of CNES and from the « Programme National de Planétologie » of INSU.

References

Allwood, A.C., Walter, M.R., Kamber, B.S., Marshall, C.P., Burch, I.W., 2006. Stromatolite reef from the Early Archaean era of Australia. Nature 441, 714–718.

Albro, P.W., 1976. In: Kolattukudy, P.E. (Ed.), Chemistry and Biochemistry of Natural Waxes. Elsevier, Amsterdam, pp. 425–427.

Beaumont, V., Robert, F., 1999. Nitrogen isotope ratios of kerogens in Precambrian cherts: a record of the evolution of atmosphere chemistry. Precam. Res. 96, 63–82.

Brasier, M.D., Green, O.R., Jephcoat, A.P., et al., 2002. Questioning the evidence for Earth's oldest fossils. Nature 416, 76–81.

Bray, E.E., Evans, E.D., 1961. Distribution of *n*-paraffins as a clue to recognition of source beds. Geochim. Cosmochim. Acta 22, 2–15.

Brocks, J.J., Logan, G.A., Buick, R., Summons, R.E., 1999. Archean molecular fossils and the early rise of eukaryotes. Science 285, 1033–1036.

Brocks, J.J., Love, G.D., Snape, C.E., Logan, G.A., Summons, R.E., Buick, R., 2003a. Release of bound aromatic hydrocarbons from late Archean and Mesoproterozoic kerogens via hydropyrolysis. Geochim. Cosmochim. Acta 67, 1521–1530.

Brocks, J.J., Buick, R., Logan, G.A., Summons, R.E., 2003b. Composition and syngeneity of molecular fossils from the 2.78 to 2.45 billion-year-old Mount Bruce Supergroup, Pilbara Craton, Western Australia. Geochim. Cosmochim. Acta 67, 4289–4319.

de Gregorio, B.T., Sharp, T.G., 2006. The structure and distribution of carbon in 3.5 Ga Apex chert: implications for the biogenicity of Earth's oldest putative microfossils. Amer. Mineral. 91, 784–789.

Durand, B., Nicaise, G., 1980. In: Durand, B. (Ed.), Kerogen. Technip, Paris, pp. 35–53.

Garcia-Ruiz, J.M., Hyde, S.T., Carnerup, A.M., Christy, A.G., van Kranendonk, M.J., Welham, N.J., 2003. Self-assembled silica-carbonate structures and detection of ancient microfossils. Science 302, 1194–1197.

Horita, J., Berndt, M.E., 1999. Abiogenic methane formation and isotopic fractionation under hydrothermal conditions. Science 285, 1055–1057.

Kato, Y., Nakamura, K., 2003. Origin and global tectonic significance of Early Archean cherts from the Marble Bar greenstone belt, Pilbara Craton, Western Australia. Precam. Res. 125, 191–243.

Marshall, C.P., Allwood, A.C., Love, G.D., Walter, R., Summons, R.E., 2006. Characterization of a 3.5 billion-year-old organic matter. Gondwana Res. 10, 393–394.

Marshall, C.P., Love, G.D., Snape, C.E., Hill, A.C., Allwood, A.C., Walter, R., van Kranendonk, M.J., Bowden, S.A., Sylva, S.P., Summons, R.E., 2007. Structural characterization of kerogen in 3.4 Ga Archaean cherts from the Pilbara craton, Western Australia. Precam. Res. 155, 1–23.

McCollom, T.M., 2003. Formation of meteorite hydrocarbons from thermal decomposition of siderite ($FeCO_3$). Geochim. Cosmochim. Acta 67, 311–317.

McCollom, T.M., Seewald, J.S., 2006. Carbon isotope composition of organic compounds produced by abiotic synthesis under hydrothermal conditions. Earth Planet Sci. Lett. 243, 74–84.

Miknis, F.P., Smith, J.W., Maughan, E.K., Maciel, G.E., 1982. Nuclear magnetic resonance—a technique for direct non-destructive evaluation of source-rock potential. Amer. Assoc. Petrol. Geol. Bull. 66, 1396–1401.

Mojzsis, S.J., Arrhenius, G., McKeegan, K.D., Harrison, T.M., Nutman, A.P., Friend, C.R.L., 1996. Evidence for life on Earth before 3,800 million years ago. Nature 384, 55–59.

Pasteris, J.D., Wopenka, B., 2002. Images of the Earth's earliest fossils? Nature 420, 476–477.

Philippot, P., Van Zuilen, M., Lepot, K., Tomazo, C., Farquhar, J., van Kranendonk, M.J., 2007. Early Archean microorganisms preferred elemental sulfur, not sulfate. Science 317, 1534–1537.

Remusat, L., Derenne, S., Robert, F., 2005a. New insight on aliphatic linkages in the macromolecular organic fraction of Orgueil and Murchison meteorites through ruthenium tetroxide oxidation. Geochim. Cosmochim. Acta 69, 4377–4386.

Remusat, L., Derenne, S., Robert, F., Knicker, H., 2005b. New pyrolytic and spectroscopic data on Orgueil and Murchison insoluble organic matter: a different origin than soluble? Geochim. Cosmochim. Acta 69, 3919–3932.

Robert, F., Chaussidon, M., 2006. A palaeotemperature curve for the Precambrian oceans based on silicon isotopes in cherts. Nature 443, 969–972.

Rouzaud, J.N., Clinard, C., 2002. Quantitative high resolution transmission electron microscopy: a promising tool for carbon materials characterization. Fuel Process. Techn. 77–78, 229–235.

Rouzaud, J.N., Skrzypczak, A., Bonal, L., Derenne, S., Robert, F., Quirico, E., 2005. The high resolution transmission electron microscopy: a powerful tool for studying the organization of terrestrial and extra-terrestrial carbons. Lunar Planet. Sci. Conf. Abstracts.

Rushdi, A.I., Simoneit, B.R.T., 2001. Lipid formation by aqueous Fisher–Tropsh type synthesis over a temperature range of 100–400 °C. Orig. Life Evol. Biosph. 31, 103–118.

Salmon, V., Derenne, S., Lallier-Verges, E., Connan, J., Kahn-Harari, A., Largeau, C., 2003. Origin of compositional differences in organic matter abundance and oil potential of cherty and clayey Cenomanian black levels in the Umbria-Marche basin (Italy). Org. Geochem. 34, 1237–1245.

Schidlowski, M., 2001. Carbon isotopes as biogeochemical recorders of life over 3.8 Ga of Earth history: evolution of a concept. Precambrian Res. 106, 117–134.

Schopf, J.W., 1993. Microfossils of the early Archean apex chert—new evidence of the antiquity of life. Science 260, 640–646.

Schopf, J.W., Kudryavtsev, A.B., Agresti, D.G., Wdowiak, T.J., Czaja, A.D., 2002. Laser-Raman imagery of Earth's earliest fossils. Nature 416, 73–76.

Sephton, M.A., Love, G.D., Watson, J.S., Verchovsky, A.B., Wright, I.P., Snape, C.E., Gilmour, I., 2004. Hydropyrolysis of insoluble carbonaceous matter in the Murchison meteorite: new insights into its macromolecular structure. Geochim. Cosmochim. Acta 68, 1385–1393.

Shen, Y., Buick, R., 2004. The antiquity of microbial sulfate reduction. Earth-Sci. Rev. 64, 243–272.

Sinninghe Damsté, J.S., Eglinton, T.I., de Leeuw, J.W., Schenck, P.A., 1989. Organic sulphur in macromolecular sedimentary organic matter: I. Structure and origin of sulphur-containing moieties in kerogen, asphaltenes and coal as revealed by flash pyrolysis. Geochim. Cosmochim. Acta 53, 873–889.

Tice, M.M., Lowe, D.R., 2006. The origin of carbonaceous matter in pre-3.0 Ga greenstone terrains: a review and new evidence from the 3.42 Ga Buck Reef Chert. Earth-Sci. Rev. 76, 259–300.

van Kranendonk, M.J., 2006. Volcanic degassins, hydrothermal circulation and flourishing of early life on Earth: a review of the evidence from c. 3490–3420 Ma rocks of the Pilbara Supergroup, Pilbara Craton, Western Australia. Earth-Sci. Rev. 74, 197–240.

Van Kranendonk, M.J., Hickman, A.H., Smithies, R.H., Nelson, D.R., Pike, G., 2002. Geology and tectonic of the North Pilbara Terrain, Pilbara Craton, Western Australia. Econ. Geol. 97, 695–732.

Van Zuilen, M., Lepland, A., Arrhenius, G., 2002. Reassessing the evidence for the earliest traces of life. Nature 418, 627–630.

Walter, M.R., Hofmann, H.J., Schopf, J.W., 1983. In: Schopf, J.W. (Ed.), Earth's Earliest Biosphere. Its Origin and Evolution. Princeton University Press, Princeton, p. 397.

Wedeking, K.W., Hayes, J.M., 1983. Carbonization of Precambrian kerogens. In: Bjoroy, M. (Ed.), Advances in Geochemistry, pp. 546–553.

Résumé présentation Michel GONDRAN du 8 avril 2013

L'action d'Euler-Lagrange $S_{cl}(x,t;x_0)$ utilisée dans tous les cours de mécanique classique, relie une particule issue d'un point x_0 à l'instant initial à sa position x à l'instant t. Elle est liée à l'action d'Hamilton-Jacobi par l'équation

$$S(x, t) = \min_{x_0}(S_0(x_0) + S_{cl}(x, t; x_0))$$

où le minimum est pris sur l'ensemble des positions initiales x_0.

Cette équation est l'analogue en mécanique classique de l'intégrale de chemin de Feynman qui relie en mécanique quantique la fonction d'onde à l'action classique. C'est une intégrale dans l'analyse Minplus que nous avons introduit en 1996, que nous appelons l'intégrale de chemin Minplus. Elle va avoir un rôle déterminant dans l'étude de la convergence de la mécanique quantique vers la mécanique classique.

On peut montrer que l'action d'Euler-Lagrange utilise les causes finales et répond à un problème posé par un observateur : « *si une particule issue de x_0 à l'instant initial arrive en x à l'instant t, quelle est sa vitesse initiale v_0* ? »

L'action d'Hamilton-Jacobi n'utilise pas les causes finales et correspond au problème résolu par la Nature.

BIBLIOGRAPHIE

M. Gondran, A. Gondran, "*Discerned and non-discerned particles in classical mechanics and convergence of quantum mechanics to classical mechanics*", Annales de la Fondation Louis de Broglie, vol. 36, 2011.

M. Gondran, A. Gondran, "*The two limits of the Schrödinger equation in the semi-classical approximation: discerned and non-discerned particles in classical mechanics* ", Foundations of Probability and Physics-6 (Växjö, Sweden, Juin 2011), AIP Conf. Proc. 1424, pp.111-115 (2012).

M. Gondran, S. Lepaul, « *Indiscernability and Mean Field, a Base of Quantum Interaction* », in "**Quantum Interaction-6th International Symposium**" (Paris, France, June 27-29, 2012) , Springer, 2012.

M. Gondran, A. Gondran, "*From interpretation of the three classical mechanics actions to the wave function in quantum mechanics*", 2nd International Conference on Theoretical Physics (Moscow, July 2012), dans Quantum Computers and Computing, vol. 12, n°1, 17-25 (2012).

The Euler-Lagrange and Hamilton-Jacobi actions and the principle of least action

Michel Gondran

*University Paris Dauphine, Lamsade, 75 016 Paris, France**

Abstract

We recall the main properties of the classical action of Euler-Lagrange $S_{cl}(\mathbf{x}, t; \mathbf{x}_0)$, which links the initial position $\mathbf{x}_0$ and its position $\mathbf{x}$ at time t, and of the Hamilton-Jacobi action, which connects a family of particles of initial action $S_0(\mathbf{x})$ to their various positions $\mathbf{x}$ at time t.

Mathematically, the Euler-Lagrange action can be considered as the elementary solution of the Hamilton-Jacobi equation in a new branch of nonlinear mathematics, the Minplus analysis. Physically, we show that, contrary to the Euler-Lagrange action, the Hamilton-Jacobi action satisfies the principle of least action. It is a clear answer on the interpretation of this principle. Finally, we use the relation-ship between the Hamilton-Jacobi and Euler-Lagrange actions to study the convergence of quantum mechanics, when the Planck constant tends to 0, for a particular class of quantum systems, the statistical semiclassical case.

I. INTRODUCTION

In 1744, Pierre-Louis Moreau de Maupertuis (1698-1759) introduced the action and the principle of least action into classical mechanics:[1] "*Nature, in the production of its effects, does so always by the simplest means [...] the path it takes is the one by which the quantity of action is the least,*" and in 1746, he states:[2] "*This is the principle of least action, a principle so wise and so worthy of the supreme Being, and intrinsic to all natural phenomena [...] When a change occurs in Nature, the quantity of action necessary for change is the smallest possible. The quantity of action is the product of the mass of the body times its velocity and the distance it moves.*" Maupertuis understood that, under certain conditions, Newton's equations are equivalent to the fact that a quantity, which he calls the action, is minimal. Euler,[3] Lagrange,[4] Hamilton,[5] Jacobi[6] and others, will make this principle of least action the most powerful tool to discover the laws of nature.[7,8] It allows, with the same approach, to determine both the equations of particle motion (if we minimize on the trajectories) and the laws of nature (if we minimize on the parameters defining the fields).

However, for the trajectories of particles, this principle is a problem for many scientists as recalled by Henri Poincaré, who was nonetheless one of its major users:[9] "*The very statement of the principle of least action has something shocking to the mind. To go from one point to another one, a material molecule, taken away from the action of any force, but constrained to move on a surface, will follow the geodesic line, i.e. the shortest path. It seems that this molecule knows the point one wants to lead it to, that it anticipates the time needed to reach it along such or such path, and then chooses the most convenient path. In a sense, the statement presents this molecule as a free animated being. It is clear that it would be better to replace it by a less shocking statement where, as philosophers would say, the final causes would not appear to replace the efficient ones.*"

We will see that the difficulties of interpretation of the action come from the existence of two actions corresponding to two different boundary conditions: the classical action (or Euler-Lagrange action) $S_{cl}(\mathbf{x}, t; \mathbf{x}_0)$, which links the initial position $\mathbf{x}_0$ and its position $\mathbf{x}$ at time t, and the Hamilton-Jacobi action $S(\mathbf{x}, t)$, which links a family of particles of initial action $S_0(\mathbf{x})$ to their various positions $\mathbf{x}$ at time t. In the Euler-Lagrange case, the initial velocity is unknown and in the Hamilton-Jacobi case, the initial position is unknown.

In section 2, we recall the main properties of Euler-Lagrange and Hamilton-Jacobi ac-

tions. In section 3, we see that the Euler-Lagrange action can be considered as the elementary solution of the Hamilton-Jacobi equation in a new branch of nonlinear mathematics, the Minplus analysis. In section 4, we show that the Hamilton-Jacobi action satisfies the principle of least action, contrary to the Euler-Lagrange action, giving a response to the scientists' embarrassment concerning the interpretation of this principle. Finally, in section 5, we use the relation between the Hamilton-Jacobi and Euler-Lagrange actions to study the convergence of quantum mechanics, when the Planck constant tends to 0, for a particular class of quantum systems, the statistical semiclassical case.

II. THE EULER-LAGRANGE AND HAMILTON-JACOBI ACTIONS

Let us consider a system evolving from the position $\mathbf{x}_0$ at initial time to the position $\mathbf{x}$ at time t; let $\mathbf{x}$(s) and $\mathbf{u}$(s) be its position and its velocity at each time $s \in [0,t]$. We have:

$$\frac{d\mathbf{x}(s)}{ds} = \mathbf{u}(s) \quad \text{for } s \in [0,t] \tag{1}$$

$$\mathbf{x}(0) = \mathbf{x}_0, \quad \mathbf{x}(t) = \mathbf{x}. \tag{2}$$

If $L(\mathbf{x}, \dot{\mathbf{x}}, t)$ is the Lagrangian of the system, the Euler-Lagrange action functional is defined by

$$J_{EL}(\mathbf{u}(.)) = \int_0^t L(\mathbf{x}(s), \mathbf{u}(s), s)ds \tag{3}$$

where the evolution of $\mathbf{x}(s)$ depends on $\mathbf{u}(s)$ through equations (1) (2).

When the two positions $\mathbf{x}_0$ and $\mathbf{x}$ are given, *the Euler-Lagrange action* $S_{cl}(\mathbf{x}, t; \mathbf{x}_0)$ is the function which realizes the minimum (or more generally an extremum[10]) of the Euler-Lagrange action on the velocity field $\mathbf{u}(.)$ for all trajectories from $(\mathbf{x}_0, 0)$ to $(\mathbf{x}$,t):

$$S_{cl}(\mathbf{x}, t; \mathbf{x}_0) = \min_{\mathbf{u}(.)} J_{EL}(\mathbf{u}(.)) = \min_{\mathbf{u}(s), 0 \le s \le t} \left\{ \int_0^t L(\mathbf{x}(s), \mathbf{u}(s), s)ds \right\}, \tag{4}$$

the minimum of (4) is taken on the continuous controls $\mathbf{u}(s)$, $s \in [0,t]$, with the state $\mathbf{x}(s)$ given by the equations (1)(2).

The solution $(\widetilde{\mathbf{u}}(s), \widetilde{\mathbf{x}}(s))$ of (4), if the Lagrangian $L(\mathbf{x}, \dot{\mathbf{x}}, t)$ is twice differentiable, satisfies the Euler-Lagrange equations on the interval $[0,t]$:[11]

$$\frac{d}{ds}\frac{\partial L}{\partial \dot{\mathbf{x}}}(\mathbf{x}(s), \dot{\mathbf{x}}(s), s) - \frac{\partial L}{\partial \mathbf{x}}(\mathbf{x}(s), \dot{\mathbf{x}}(s), s) = 0 \qquad (0 \le s \le t) \tag{5}$$

$$\mathbf{x}(0) = \mathbf{x}_0, \quad \mathbf{x}(t) = \mathbf{x}. \tag{6}$$

For a nonrelativistic particle in a linear potential field with the Lagrangian $L(\mathbf{x},\dot{\mathbf{x}},t) = \frac{1}{2}m\dot{\mathbf{x}}^2 + \mathbf{K}.\mathbf{x}$, the equation (5) yields $\frac{d}{ds}(m\dot{\mathbf{x}}(s)) - \mathbf{K} = 0$. The trajectory which minimizes the action is $\widetilde{\mathbf{x}}(s) = \mathbf{x}_0 + \frac{s}{t}(\mathbf{x}-\mathbf{x}_0) - \frac{\mathbf{K}}{2m}ts + \frac{\mathbf{K}}{2m}s^2$, and the Euler-Lagrange action is equal to $S_{cl}(\mathbf{x},t;\mathbf{x}_0) = m\frac{(\mathbf{x}-\mathbf{x}_0)^2}{2t} + \frac{K.(\mathbf{x}+\mathbf{x}_0)}{2}t - \frac{K^2}{24m}t^3$.

More generally, in the case of a nonrelativistic particle with the Lagrangian $L(\mathbf{x},\mathbf{v},t) = \frac{1}{2}m\mathbf{v}^2 - V(\mathbf{x},t)$, the Euler-Lagrange action yields the velocities of the two extremities of the trajectory:

$$\mathbf{v}_0 = \dot{\mathbf{x}}(o) = -\frac{1}{m}\frac{\partial S_{cl}}{\partial \mathbf{x}_0}(\mathbf{x},t;\mathbf{x}_0) \qquad and \qquad \mathbf{v}(\mathbf{x},t;\mathbf{x}_0) = \dot{\mathbf{x}}(t) = \frac{1}{m}\frac{\partial S_{cl}}{\partial \mathbf{x}}(\mathbf{x},t;\mathbf{x}_0). \tag{7}$$

For the above exemple, we find:

$$\mathbf{v}_0 = \dot{\mathbf{x}}(o) = \frac{\mathbf{x}-\mathbf{x}_0}{t} - \frac{Kt}{2m} \qquad and \qquad \mathbf{v}(\mathbf{x},t;\mathbf{x}_0) = \dot{\mathbf{x}}(t) = \frac{\mathbf{x}-\mathbf{x}_0}{t} + \frac{Kt}{2m}.$$

Let us consider now that an initial action $S_0(\mathbf{x})$ is given, then the Hamilton-Jacobi functional from x_0 is defined by:[12]

$$J_{HJ}(\mathbf{u}(.)) = S_0(\mathbf{x}_0) + \int_0^t L(\mathbf{x}(s),\mathbf{u}(s),s)\ ds = S_0(\mathbf{x}_0) + J_{EL}(\mathbf{u}(.)) \tag{8}$$

where the evolution of $\mathbf{x}(s)$ depends on $\mathbf{u}(s)$ through equations (1) (2).

The Hamilton-Jacobi action $S(\mathbf{x},t)$ is the function which realizes the minimum of the Hamilton-Jacobi action functional on the trajectories arriving in $\mathbf{x}$ at time t:

$$S(\mathbf{x},t) = \min_{\mathbf{x}_0;\mathbf{u}(.)} J_{HJ}(\mathbf{u}\,(.)) = \min_{\mathbf{x}_0;\mathbf{u}(s),0\le s\le t}\left\{S_0\,(\mathbf{x}_0) + \int_0^t L(\mathbf{x}(s),\mathbf{u}(s),s)ds\right\} \tag{9}$$

the minimum of (9) is taken on all initial positions $\mathbf{x}_0$, on the controls $\mathbf{u}(s)$, $s\in[0,t]$, with the state $\mathbf{x}(s)$ given by the equations (1)(2).

Because the term $S_0(\mathbf{x}_0)$ has no effect in (9) for the minimization on $\mathbf{u}(s)$, we deduce the following relation between the Hamilton-Jacobi action and Euler-Lagrange action:

$$S(\mathbf{x},t) = \min_{\mathbf{x}_0}(S_0\,(\mathbf{x}_0) + S_{cl}(\mathbf{x},t;\mathbf{x}_0)). \tag{10}$$

For a particle in a linear potential $V(\mathbf{x}) = -\mathbf{K}.\mathbf{x}$ with the initial action $S_0(\mathbf{x}) = m\mathbf{v}_0\cdot\mathbf{x}$, the Hamilton-Jacobi action is equal to $S\,(\mathbf{x},t) = m\mathbf{v}_0\cdot\mathbf{x} - \frac{1}{2}m\mathbf{v}_0^2t + \mathbf{K}.\mathbf{x}t - \frac{1}{2}\mathbf{K}.\mathbf{v}_0t^2 - \frac{\mathbf{K}^2t^3}{6m}$.

The Hamilton-Jacobi action $S(\mathbf{x},t)$ defined by (9) can be decomposed into

$$S(\mathbf{x},t) = \min_{\mathbf{x}_0;\mathbf{u}(s),0\le s\le t}\left\{S_0\,(\mathbf{x}_0) + \int_0^{t-dt} L(\mathbf{x}(s),\mathbf{u}(s),s)ds + \int_{t-dt}^{t} L(\mathbf{x}(s),\mathbf{u}(s),s)ds\right\}$$

and then satisfies the optimality equation:

$$S(\mathbf{x},t)=\min_{\mathbf{u}(s),t-dt\leq s\leq t}\left\{S(\mathbf{x}-\int_{t-dt}^{t}\mathbf{u}(s)ds,t-dt)+\int_{t-dt}^{t}L(\mathbf{x}(s),\mathbf{u}(s),s)ds\right\}.$$

If we assume S to be differentiable for $\mathbf{x}$ and t, L differentiable for $\mathbf{x}$, $\mathbf{u}$ and t, and $\mathbf{u}$(s) continuous, this equation becomes:

$$0=\min_{\mathbf{u}(t)}\left\{-\frac{\partial S}{\partial \mathbf{x}}(\mathbf{x},t)\,\mathbf{u}(t)\,dt-\frac{\partial S}{\partial \mathbf{t}}(\mathbf{x},t)\,dt+L(\mathbf{x},\mathbf{u}(t),t)dt+\circ(dt)\right\}$$

and in dividing by dt and letting dt tend towards 0^{+},

$$\frac{\partial S}{\partial \mathbf{t}}(\mathbf{x},t)=\min_{\mathbf{u}}\left\{L(\mathbf{x},\mathbf{u},t)-\mathbf{u}\cdot\frac{\partial S}{\partial \mathbf{x}}(\mathbf{x},t)\right\}.$$

We recall that at all convex functions $f(\mathbf{u}):\mathbf{u}\in\mathbb{R}^n\to\mathbb{R}$ we can associate its *Fenchel-Legendre transform* $\widehat{f}(\mathbf{r}):\mathbf{r}\in\mathbb{R}^n\to\mathbb{R}$ defined by $\widehat{f}(\mathbf{r})=\max_{\mathbf{u}\in\mathbb{R}^n}(\mathbf{r}\cdot\mathbf{u}-f(\mathbf{u}))$. The Hamiltonian $H(\mathbf{x},\mathbf{p},t)$ is then the Fenchel-Legendre transform of the Lagrangian $L(\mathbf{x},\mathbf{u},t)$ for the variable $\mathbf{u}$.

Then, the Hamilton-Jacobi action satisfies the Hamilton-Jacobi equations:

$$\frac{\partial S}{\partial t}+H(\mathbf{x},\frac{\partial S}{\partial \mathbf{x}},t)=0 \tag{11}$$

$$S(\mathbf{x},0)=S_0(\mathbf{x}). \tag{12}$$

For the Lagrangian $L(\mathbf{x},\dot{\mathbf{x}},t)=\frac{1}{2}m\dot{\mathbf{x}}^2-V(\mathbf{x},t)$, $H(\mathbf{x},\nabla S,t)=\max_{\mathbf{v}}(\mathbf{v}.\nabla S-\frac{1}{2}m\mathbf{v}^2+V(\mathbf{x},t))$, we have for the optimum $m\mathbf{v}=\nabla S$. We deduce $H(\mathbf{x},\nabla S)=\frac{1}{2m}(\nabla S)^2+V(\mathbf{x},t)$ and the well known result:

The velocity of a nonrelativistic classical particle in a potential field is given for each point $(\mathbf{x},t)$ *by*:

$$\mathbf{v}(\mathbf{x},t)=\frac{\nabla S(\mathbf{x},t)}{m} \tag{13}$$

where $S(\mathbf{x},t)$ *is the Hamilton-Jacobi action, a solution to the Hamilton-Jacobi equations:*

$$\frac{\partial \mathcal{S}}{\partial t}+\frac{1}{2m}(\nabla\mathcal{S})^2+V(\mathbf{x},t)=0 \tag{14}$$

$$\mathcal{S}(\mathbf{x},0)=\mathcal{S}_0(\mathbf{x}). \tag{15}$$

Equation (13) shows that the solution $S(\mathbf{x},t)$ to the Hamilton-Jacobi equations yields the velocity field for each point $(\mathbf{x},t)$ from the velocity field $\frac{\nabla S_0(\mathbf{x})}{m}$ at initial time. In particular, if at initial time, we know the initial position $\mathbf{x}_{init}$ of a particle, its velocity at this time is

equal to $\frac{\nabla S_0(\mathbf{x}_{init})}{m}$. From the solution $S(\mathbf{x},t)$ to the Hamilton-Jacobi equations, we deduce with (13) the trajectories of the particle. The Hamilton-Jacobi action $S(\mathbf{x},t)$ is then a field which "pilots" the particle.

Let us recall how the Hamilton-Jacobi action allows to find Newton's second law of motion.[13] First, we take the gradient of the Hamilton-Jacobi equation (14) $\frac{\partial^2 \mathcal{S}}{\partial t \partial x_i} + \frac{1}{m}\sum_j \frac{\partial^2 \mathcal{S}}{\partial x_i \partial x_j}\frac{\partial \mathcal{S}}{\partial x_j} + \frac{\partial V}{\partial x_i} = 0$. Second, we remark that $\frac{d}{dt}\left(\frac{\partial \mathcal{S}}{\partial x_i}\right) = \frac{\partial^2 \mathcal{S}}{\partial t \partial x_i} + \sum_j \frac{\partial^2 \mathcal{S}}{\partial x_i \partial x_j} v_j$ and with the equation (13) where $m\mathbf{v} = \nabla S$, we conclude $\frac{d}{dt}(m\mathbf{v}) = -\nabla V$.

III. THE EULER-LAGRANGE AND HAMILTON-JACOBI ACTIONS IN MINPLUS ANALYSIS

There is a new branch of mathematics, the Minplus analysis, which studies nonlinear problems through a linear approach, cf. Maslov[14,15] and Gondran[16,17]. The idea is to substitute the usual scalar product $\int_X f(x)g(x)dx$ by the Minplus scalar product:

$$(f,g) = \inf_{x\in X}\{f(x) + g(x)\} \tag{16}$$

In the scalar product we replace the field of the real number $(\mathbb{R},+,\times)$ with the algebraic structure *Minplus* $(\mathbb{R}\cup\{+\infty\},\min,+)$, i.e. the set of real numbers (with the element infinity $\{+\infty\}$) endowed with the operation Min (minimum of two reals), which remplaces the usual addition, and with the operation + (sum of two reals), which remplaces the usual multiplication. The element $\{+\infty\}$ corresponds to the neutral element for the operation Min, $\text{Min}(\{+\infty\},a) = a\ \forall a \in \mathbb{R}$.

This approach bears a close similarity to *the theory of distributions for the nonlinear case*; here, the operator is "linear" and continuous with respect to the Minplus structure, though *nonlinear* with respect to the classical structure $(\mathbb{R},+,\times)$. In this Minplus structure, the Hamilton-Jacobi equation is linear, because if $S_1(\mathbf{x},t)$ and $S_2(\mathbf{x},t)$ are solutions to (14), then $\min\{\lambda + S_1(\mathbf{x},t), \mu + S_2(\mathbf{x},t)\}$ is also solution to the Hamilton-Jacobi equation (14).

The analogue to the Dirac distribution $\delta(\mathbf{x})$ in Minplus analysis is the nonlinear distribution $\delta_{\min}(\mathbf{x}) = \{0\ if\ \mathbf{x} = \mathbf{0}, +\infty\ if\ not\}$. With this nonlinear Dirac distribution, we can define elementary solutions as in classical distribution theory. In particular, we have:

The classical Euler-Lagrange action $S_{cl}(\boldsymbol{x},t;\boldsymbol{x}_0)$ is the elementary solution to the

Hamilton-Jacobi equations (11)(12) in the Minplus analysis with the initial condition

$$S(\mathbf{x},0) = \delta_{\min}(\mathbf{x}-\mathbf{x}_0) = \{0 \;\; if \;\; \mathbf{x}=\mathbf{x}_0, \;\; +\infty \;\; if \; not\}.$$

The Hamilton-Jacobi action $S(\mathbf{x},t)$ is then given by the Minplus integral:

$$S(\mathbf{x},t) = \inf_{\mathbf{x}_0}\{S_0(\mathbf{x}_0) + S_{cl}(\mathbf{x},t;\mathbf{x}_0)\}$$

in analogy with the solution of the heat transfer equation given by the classical integral:

$$S(x,t) \;=\; \int S_0\,(x_0)\,\frac{1}{2\sqrt{\pi t}}\;e^{-\dfrac{(x-x_0)^2}{4t}}\,dx_0.$$

In this Minplus analysis, the Legendre-Fenchel transform is the analogue to the Fourier transform. This transform is known to have many applications in Physics: this is the one which sets the correspondence between the Lagrangian and the Hamiltonian of a physical system; which sets the correspondence between microscopic and macroscopic models; which is also at the basis of multifractal analysis relevant to modeling turbulence in fluid mechanics.[17]

IV. THE PRINCIPLE OF LEAST ACTION

Equation (9) shows that, among the trajectories which can reach $(\mathbf{x},t)$ from a position at the initial time whose initial velocity field is known, Nature chooses the velocity which minimizes (or realizes the extremum) of the Hamilton-Jacobi functional. Then, the principle of least action defines the velocity field at time t: $(\mathbf{v}(\mathbf{x},t) = \frac{\nabla S(\mathbf{x},t)}{m})$. For the Lagrangian $L(\mathbf{x},\dot{\mathbf{x}},t) = \frac{1}{2}m\dot{\mathbf{x}}^2 - \mathbf{K}.\mathbf{x}$, we find $\mathbf{v}(\mathbf{x},t) = \mathbf{v}_0 + \mathbf{K}t/m$. The Hamilton-Jacobi action $S(\mathbf{x},t)$ does not solve only a given problem with a single initial condition $\left(\mathbf{x}_0, \frac{\nabla S_0(\mathbf{x}_0)}{m}\right)$, but a set of problems with an infinity of initial conditions, all the couples $\left(\mathbf{y}, \frac{\nabla S_0(\mathbf{y})}{m}\right)$.

Does the Euler-Lagrange action correspond to the principle of least action? The answer seems positive from equation (4). But in fact, in the absence of an initial velocity field as in the Hamilton-Jacobi action, the Euler-Lagrange action answers a problem posed by the observer, and not by Nature: "If we see that a particle in $\mathbf{x}_0$ at the initial time arrives in $\mathbf{x}$ at time t, what was its initial velocity $\mathbf{v}_0$?" To solve this problem, the observer must solve the Euler-Lagrange equations (5,6) which are difficult because they concern the entire

trajectory. We have seen that this velocity is given by equation (7): $\mathbf{v}_0 = -\frac{1}{m}\frac{\partial S_{cl}}{\partial \mathbf{x}_0}(\mathbf{x}, t; \mathbf{x}_0)$. This is an *a posteriori* point of view.

Contrary to the Euler-Lagrange action, the Hamilton-Jacobi action answers the following problem:"If we know the action (or the velocity field) at the initial time, can we determine the action (or the velocity field) at each later time?" This problem is solved from time to time by the evolution equation (11) or (14) which is local. This is an *a priori* point of view. It is the problem solved by Nature with the principle of least action. The Euler-Lagrange action, which is an elementary solution to the Hamilton-Jacobi equation, seems to satisfy this principle. But, only the Hamilton-Jacobi action satisfies the principle of least action. It is a clear answer to the Poincaré question on the interpretation of this principle.

V. LIMIT OF THE SCHRÖDINGER EQUATION IN THE STATISTICAL SEMI-CLASSICAL CASE

Equation (10) between the Hamilton-Jacobi and Euler-Lagrange actions will allow us to study the convergence of quantum mechanics, when the Planck constant tends to 0, for a particular class of quantum systems.

Let us consider the wave function solution to the Schrödinger equation $\Psi(\mathbf{x}, t)$:

$$i\hbar\frac{\partial \Psi}{\partial t} = -\frac{\hbar^2}{2m}\triangle\Psi + V(\mathbf{x}, t)\Psi \tag{17}$$

$$\Psi(\mathbf{x}, 0) = \Psi_0(\mathbf{x}). \tag{18}$$

With the variable change $\Psi(\mathbf{x}, t) = \sqrt{\rho^\hbar(\mathbf{x}, t)}\exp(i\frac{S^\hbar(\mathbf{x},t)}{\hbar})$, the quantum density $\rho^\hbar(\mathbf{x}, t)$ and the quantum action $S^\hbar(\mathbf{x}, t)$ depend on the parameter $\hbar$. The Schrödinger equation can be decomposed into Madelung equations[18] (1926):

$$\frac{\partial S^\hbar(\mathbf{x}, t)}{\partial t} + \frac{1}{2m}(\nabla S^\hbar(\mathbf{x}, t))^2 + V(\mathbf{x}, t) - \frac{\hbar^2}{2m}\frac{\triangle\sqrt{\rho^\hbar(\mathbf{x}, t)}}{\sqrt{\rho^\hbar(\mathbf{x}, t)}} = 0 \tag{19}$$

$$\frac{\partial \rho^\hbar(\mathbf{x}, t)}{\partial t} + div(\rho^\hbar(\mathbf{x}, t)\frac{\nabla S^\hbar(\mathbf{x}, t)}{m}) = 0 \qquad \forall(\mathbf{x}, t) \tag{20}$$

with initial conditions

$$\rho^\hbar(\mathbf{x}, 0) = \rho_0^\hbar(\mathbf{x}) \qquad and \qquad S^\hbar(\mathbf{x}, 0) = S_0^\hbar(\mathbf{x}). \tag{21}$$

Here, we study the convergence of the density $\rho^\hbar(\mathbf{x}, t)$ and the action $S^\hbar(\mathbf{x}, t)$, when $\hbar$ tends to 0, for a particular preparation of the particles. A quantum system is prepared in *the*

statistical semi-classical case[19,20] if its initial probability density $\rho_0^\hbar(\mathbf{x})$ and its initial action $S_0^\hbar(\mathbf{x})$ are regular functions $\rho_0(\mathbf{x})$ and $S_0(\mathbf{x})$ not depending on $\hbar$, and its interaction with the potential field $V(\mathbf{x},t)$ can be described classically. It is the case of a set of particles that are non-interacting and prepared in the same way: a free particles beam in a linear potential, an electronic or C_{60} beam in the Young's slits diffraction, an atomic beam in the Stern and Gerlach experiment. Then, we have the following result:[19,20]

For particles in the statistical semi-classical case, the probability density $\rho^\hbar(\boldsymbol{x},t)$ and the action $S^\hbar(\boldsymbol{x},t)$, solutions to the Madelung equations (19)(20)(21), converge, when $\hbar \to 0$, to the classical density $\rho(\boldsymbol{x},t)$ and the classical action $S(\boldsymbol{x},t)$, solutions to the statistical Hamilton-Jacobi equations:

$$\frac{\partial S(\mathbf{x},t)}{\partial t} + \frac{1}{2m}(\nabla S(\mathbf{x},t))^2 + V(\mathbf{x},t) = 0 \tag{22}$$

$$\frac{\partial \rho(\mathbf{x},t)}{\partial t} + div\left(\rho(\mathbf{x},t)\frac{\nabla S(\mathbf{x},t)}{m}\right) = 0 \qquad \forall(\mathbf{x},t) \tag{23}$$

$$\rho(\mathbf{x},0) = \rho_0(\mathbf{x}) \qquad and \qquad S(\mathbf{x},0) = S_0(\mathbf{x}). \tag{24}$$

We will demonstrate in the case where the wave function $\Psi(\mathbf{x},t)$ at time t is written as a function of the initial wave function $\Psi_0(\mathbf{x})$ by the Feynman paths integral formula[22] (p. 58):

$$\Psi(\mathbf{x},t) = \int F(t,\hbar)\exp(\frac{i}{\hbar}S_{cl}(\mathbf{x},t;\mathbf{x}_0)\Psi_0(\mathbf{x}_0)d\mathbf{x}_0$$

where $F(t,\hbar)$ is an independent function of $\mathbf{x}$ and of $\mathbf{x}_0$ and where $S_{cl}(\mathbf{x},t;\mathbf{x}_0)$ is the classical action. In the statistical semi-classical case, the wave function is written $\Psi(\mathbf{x},t) = F(t,\hbar)\int\sqrt{\rho_0(\mathbf{x}_0)}\exp(\frac{i}{\hbar}(S_0(\mathbf{x}_0)+S_{cl}(\mathbf{x},t;\mathbf{x}_0))d\mathbf{x}_0$. The theorem of the stationary phase[22] shows that, if $\hbar$ tends towards 0, we have $\Psi(\mathbf{x},t) \sim \exp(\frac{i}{\hbar}min_{\mathbf{x}_0}(S_0(\mathbf{x}_0)+S_{cl}(\mathbf{x},t;\mathbf{x}_0))$, that is to say that the quantum action $S^h(\mathbf{x},t)$ converges to the function

$$S(\mathbf{x},t) = min_{\mathbf{x}_0}(S_0(\mathbf{x}_0)+S_{cl}(\mathbf{x},t;\mathbf{x}_0))$$

which is the solution to the Hamilton-Jacobi equation (22) with the initial condition (24). Moreover, as the quantum density $\rho^h(\mathbf{x},t)$ verifies the continuity equation (20), we deduce, since $S^h(\mathbf{x},t)$ tends towards $S(\mathbf{x},t)$, that $\rho^h(x,t)$ converges to the classical density $\rho(\mathbf{x},t)$, which satisfies the continuity equation (23). We obtain both announced convergences.

If we consider the system with initial conditions $\rho_0^\hbar(\mathbf{x}) = \rho_0(\mathbf{x}) = (2\pi\sigma_0^2)^{-\frac{3}{2}}e^{-\frac{(\mathbf{x}-\zeta_0)^2}{2\sigma_0^2}}$ and $S_0^\hbar(\mathbf{x}) = S_0(\mathbf{x}) = m\mathbf{v}_0\cdot\mathbf{x}$ in a linear potential field $V(\mathbf{x}) = -\mathbf{K}\cdot\mathbf{x}$, where σ_0, $\mathbf{v}_0$, ζ_0 and

$\mathbf{K}$ are constants independent of $\hbar$, the density $\rho^{\hbar}(\mathbf{x},t)$ and the action $S^{\hbar}(\mathbf{x},t)$ are equal to[21] $\rho^{\hbar}(\mathbf{x},t) = (2\pi\sigma_{\hbar}^2(t))^{-\frac{3}{2}} exp - \frac{\left(\mathbf{x}-\zeta_0-\mathbf{v}_0 t-\mathbf{K}\frac{t^2}{2m}\right)^2}{2\sigma_{\hbar}^2(t)}$ and

$$S^{\hbar}(\mathbf{x},t) = -\frac{3\hbar}{2} t g^{-1}(\hbar t/2m\sigma_0^2) - \frac{1}{2} m\mathbf{v}_0^2 t + m\mathbf{v}_0\cdot\mathbf{x} + \mathbf{K}\cdot\mathbf{x}t - \frac{1}{2}\mathbf{K}\cdot\mathbf{v}_0 t^2 - \frac{\mathbf{K}^2 t^3}{6m} + \frac{\left(\mathbf{x}-\zeta_0-\mathbf{v}_0 t-\mathbf{K}\frac{t^2}{2m}\right)^2 \hbar^2 t}{8m\sigma_0^2\sigma_{\hbar}^2(t)}$$

with $\sigma_{\hbar}(t) = \sigma_0\left(1+(\hbar t/2m\sigma_0^2)^2\right)^{\frac{1}{2}}$. When $\hbar \to 0$, $\sigma_{\hbar}(t)$ converges to σ_0 and the density $\rho^{\hbar}(\mathbf{x},t)$ and the action $S^{\hbar}(\mathbf{x},t)$ converge to $\rho(\mathbf{x},t) = (2\pi\sigma_0^2)^{-\frac{3}{2}} e^{-\frac{\left(\mathbf{x}-\zeta_0-\mathbf{v}_0 t-\mathbf{K}\frac{t^2}{2m}\right)^2}{2\sigma_0^2}}$ and $S(\mathbf{x},t) = -\frac{1}{2}m\mathbf{v}_0^2 t + m\mathbf{v}_0\cdot\mathbf{x} + \mathbf{K}\cdot\mathbf{x}t - \frac{1}{2}\mathbf{K}\cdot\mathbf{v}_0 t^2 - \frac{\mathbf{K}^2 t^3}{6m}$ which are solutions to statistical Hamilton-Jacobi equations (22)(23)(24).

The statistical Hamilton-Jacobi equations correspond to a set of independent classical particles, in a potential field $V(\mathbf{x},t)$, and for which we only know at the initial time the probability density $\rho_0(\mathbf{x})$ and the velocity $\mathbf{v}(\mathbf{x}) = \frac{\nabla S_0(\mathbf{x},t)}{m}$. These particles are not indistinguishable because, if their initial positions are known, their trajectories will also be known. Nevertheless, these particles will have the same properties as the indistinguishable ones. Thus, if the initial density $\rho_0(\mathbf{x})$ is given, and one randomly chooses N particles, the N! permutations are strictly equivalent and do not correspond to the same configuration as for indistinguishable particles.

For particles prepared in the statistical semi-classical case, the uncertainity about the position of a quantum particle corresponds to an uncertainity about the position of a classical particle, whose initial density alone has been defined. *In classical mechanics, this uncertainity is removed by giving the initial position of the particle. It would not be logical not to do the same in quantum mechanics.* It is then possible to assume that for *the statistical semi-classical case*, a quantum particle is not well described by its wave function. One needs therefore to add its initial position and it becomes natural to introduce the so-called de Broglie-Bohm trajectories[23,24] with the velocity $\mathbf{v}^{\hbar}(\mathbf{x},t) = \frac{1}{m}\nabla S^{\hbar}(\mathbf{x},t)$.

VI. AKNOWLEDGEMENTS

I thank Sebastien Lepaul for these interesting and useful remarks.

---

* Electronic address: michel.gondran@polytechnique.org

[1] P.L. de Maupertuis, "Accord de différentes loix de la nature qui avaient jusqu'ici paru incompatibles", Mémoires de l'Académie Royale des Sciences (Paris,1744), p.417-426, reprint in Oeuvres, **4**, 1-23 Reprografischer Nachdruck der Ausg. Lyon (1768).

[2] P.L. de Maupertuis, "Les Loix du mouvement et du repos déduites d'un principe métaphysique", Mémoire Académie Berlin (1746), p. 267, reprint in Oeuvres, **4**, 36-38(1768).

[3] Leonhard Euler, "Methodus Inveniendi Lineas Curvas Maximi Minive Proprietate Gaudentes",(1744) Bousquet, Lausanne et Geneva. reprint in Leonhardi Euleri Opera Omnia: Series I vol 24 (1952) C. Cartheodory (ed.) Orell Fuessli,Zurich.

[4] J.L. Lagrange, *Analytic Mechanics*(*Mécanique Analytique*) Gauthier-Villars, Paris, 1888, 2nd ed., translated by V. Vagliente and A. Boissonade (Klumer Academic, Dordrecht, 2001).

[5] William Rowan Hamilton, "On a general method in dynamics, by which the study of the motions of all free systems of attracting or repelling points is reduced to the search and differentiation of one central Relation or characteristic Function," Philos. Trans; R. Soci. PartII, 247-308 (1834); "Second essay on a general method in dynamics," ibid. Part I, 95-144 (1835). Both papers are available at $\langle http///www.emis.de/classics/Hamilton/\rangle$.

[6] G.C.J. Jacobi, *Vorlesungen über Dynamik, gehalten an der Universität Königberg im Wintersemester 1842-1843*. A. Clebsch (ed.) (1866); Reimer, Berlin. Available online Oeuvres complètes volume 8 at Gallica-Math from Gallica Bibliothèque Nationale de France.

[7] R.P. Feynman, R.B. Leighton, and M. Sands, *The Feynman Lectures on Physics* (Addison-Wesley, Reading, MA, 1964), Vol. II, pp.19-8.

[8] L.D. Landau and E.M. Lifshitz, *Mechanics, Course of Theoretical Physics* (Buttreworth-Heinemann, London, 1976), 3rd ed., Vol. 1, Chap. 1. Their renaming first occured in the original 1957 Russian edition.

[9] Poincaré, *La Science et l'Hypothèse*, Flammarion, 1902, translated in *The Foundations of Sciences: Science and Hypothesis, The value of Science, Science and Method*, New York: Science

Press, 1913.

[10] C.G. Gray, and E.F. Taylor, "When action is not the least." Am. J. Phys.**75**, 434-458, 2007.

[11] J. Hanc, E. F. Taylor, and S. Tuleja, "Deriving Lagrange's equations using elementary calculus," Am. J. Phys. 72, 510 513 2004.

[12] L. C. Evans, *Partial Differential Equations*, Graduate Studies in Mathematics **19**, American Mathematical Society, p.123-124, 1998.

[13] J. Hanc, S. Tuleja, and M. Hancova, "Simple derivation of Newtonian mechanics from the principle of least action," Am. J. Phys.**71**, 386-391, 2003.

[14] V.P. Maslov and S. N. Samborskiĭ, Eds.,*Idempotent Analysis*, Advances in Soviet Mathematics, Vol. 13, Amer. Math; Soc., Providence, RI, 1992.

[15] V.N. Kolokoltsov and V.P. Maslov, *Idempotent Analysis and its applications*, Klumer Acad. Publ., 1997.

[16] M. Gondran, "Analyse MinPlus", C. R. Acad. Sci. Paris **323**, 371-375 (1996).

[17] M. Gondran et M. Minoux, *Graphs, Dioïds and Semi-rings: New models and Algorithms*, chap.7, Springer, Operations Research/Computer Science Interfaces (2008).

[18] E. Madelung,), "Quantentheorie in hydrodynamischer Form", Zeit. Phys. **40** (1926) 322-6.

[19] M. Gondran and A. Gondran, "Discerned and non-discerned particles in classical mechanics and convergence of quantum mechanics to classical mechanics", Annales de la Fondation Louis de Broglie, vol. 36, 117-135, 2011.

[20] M. Gondran and A. Gondran, "The two limits of the Schrödinger equation in the semi-classical approximation: discerned and non-discerned particles in classical mechanics ", Proceeding of AIP, Conference Foundations of Probability and Physics 6, Växjö, Sweden, june 2011, vol 1424, 2012.

[21] C. Cohen-Tannoudji, B.Diu, and F. Lalo, *Quantum Mechanics*, (Wiley, New York, 1977).

[22] R. Feynman and A. Hibbs, *Quantum Mechanics and Integrals*, McGraw-Hill, 1965.

[23] L. de Broglie, "La mécanique ondulatoire et la structure atomique de la matière et du rayonnement", J. de Phys. **8**, 225-241 (1927).

[24] D. Bohm, "A suggested interpretation of the quantum theory in terms of "hidden" variables", Phys. Rev.**85**, 166-193 (1952).

The principle of least action as interpreted by Nature and by the observer

Michel Gondran

University Paris Dauphine, 75 016 Paris, France

Abstract

In this paper, we show that the difficulties of interpretation of the principle of least action about the "final causes" or the "efficient causes" are due to the existence of two actions corresponding to two different boundary conditions: the "Euler-Lagrange action" (or classical action) and the "Hamilton-Jacobi action". We provide a novel way to look at the Hamilton-Jacobi action, which permits to better understand its difference with the Euler-Lagrange action. Then, we give a clear-cut interpretation of the principle of least action: the Hamilton-Jacobi action does not use the "final causes" and seems to be the action used by Nature; the Euler-Lagrange action uses the "final causes" and is the action used by an observer to determine retrospectively the trajectory of the particle.

Keywords: principle of least action, Euler-Lagrange action, Hamilton-Jacobi action, final causes, efficient causes

1. Introduction

In 1744, Pierre-Louis Moreau de Maupertuis (1698-1759) introduced the action and the principle of least action into classical mechanics (de Maupertuis (1744)):"*Nature, in the production of its effects, does so always by the simplest means [...] the path it takes is the one by which the quantity of action is the least,*" and in 1746, he states (de Maupertuis (1746)): "*This is the principle of least action, a principle so wise and so worthy of the supreme Being, and intrinsic to all natural phenomena [...] When a change occurs*

Email address: michel.gondran@polytechnique.org (Michel Gondran)

in Nature, the quantity of action necessary for change is the smallest possible. The quantity of action is the product of the mass of the body times its velocity and the distance it moves." Maupertuis understood that, under certain conditions, Newton's equations amounts to the minimization of a certain quantity. He dubbed this quantity as the action. Euler (Euler (1744)), Lagrange (Lagrange (1888)), Hamilton (Hamilton (1834, 1835)), Jacobi (Jacobi (1866)) and others, will turn this principle of least action into one of the most powerful tool to discover the laws of nature (Feynman et al. (1964); Landau and Lifshitz (1957)). This principle permits to determine the equations of motion of a particle (if we minimize on the trajectories) and the laws of nature (if we minimize on the parameters defining the fields).

However, when applied to the study of trajectories of particles, this principle has often been viewed as puzzling by many scholars, including Henri Poincaré, who was nonetheless one of its intensive users (Poincaré (1902)): "*The very statement of the principle of least action has something shocking to the mind. To go from one point to another one, a material molecule, taken away from the action of any force, but constrained to move on a surface, will follow the geodesic line, i.e. the shortest path. It seems that this molecule knows the point one wants to lead it to, that it anticipates the time needed to reach it along such or such path, and then chooses the most convenient path. In a sense, the statement presents this molecule as a free animated being. It is clear that it would be better to replace it by a less shocking statement where, as philosophers would say, the final causes would not appear to replace the efficient ones.*"

We will show that the difficulties of interpretation of the principle of least action about the "final causes" or the "efficient causes" come from the existence of two actions corresponding to two different boundary conditions: the "Euler-Lagrange action" (or classical action) $S_{cl}(\mathbf{x}, t; \mathbf{x}_0)$, which links the initial position $\mathbf{x}_0$ and its position $\mathbf{x}$ at time t, and the often neglected "Hamilton-Jacobi action" $S(\mathbf{x}, t)$, which relates a family of particles of initial action $S_0(\mathbf{x})$ to their various positions $\mathbf{x}$ at time t. While the Euler-Lagrange procedure entails an unknown initial velocity, the Hamilton-Jacobi method implies an unknown initial position.

In section 2, we recall the main properties of Euler-Lagrange and Hamilton-Jacobi actions. In particular, we give a new presentation of the Hamilton-Jacobi action which highlights the differences with the Euler-Lagrange action. In section 3, we respond to Poincaré by provinding an clear-cut interpretation of this principle.

2. The Euler-Lagrange and Hamilton-Jacobi actions

Let us consider a system evolving from the position $\mathbf{x}_0$ at initial time to the position $\mathbf{x}$ at time t where the variable of control $\mathbf{u}$(s) is the velocity:

$$\frac{d\mathbf{x}\,(s)}{ds} = \mathbf{u}(s) \qquad for \quad s \in [0,t] \tag{1}$$

$$\mathbf{x}(0) = \mathbf{x}_0, \qquad \mathbf{x}(t) = \mathbf{x}. \tag{2}$$

If $L(\mathbf{x}, \dot{\mathbf{x}}, t)$ is the Lagrangian of the system, when the two positions $\mathbf{x}_0$ and $\mathbf{x}$ are given, *the Euler-Lagrange action* $S_{cl}(\mathbf{x}, t; \mathbf{x}_0)$ is the function defined by:

$$S_{cl}(\mathbf{x}, t; \mathbf{x}_0) = \min_{\mathbf{u}(s), 0 \le s \le t} \int_0^t L(\mathbf{x}(s), \mathbf{u}(s), s) ds, \tag{3}$$

where the minimum (or more generally an extremum) is taken on the controls $\mathbf{u}(s)$, $s \in [0,t]$, with the state $\mathbf{x}(s)$ given by the equations (1)(2).

The solution $(\widetilde{\mathbf{x}}(s), \widetilde{\mathbf{u}}(s))$ of (3), if the Lagrangian $L(\mathbf{x}, \dot{\mathbf{x}}, t)$ is twice differentiable, satisfies the Euler-Lagrange equations on the interval $[0,t]$:

$$\frac{d}{ds}\frac{\partial L}{\partial \dot{\mathbf{x}}}(\mathbf{x}(s), \dot{\mathbf{x}}(s), s) - \frac{\partial L}{\partial \mathbf{x}}(\mathbf{x}(s), \dot{\mathbf{x}}(s), s) = 0 \qquad (0 \le s \le t) \tag{4}$$

$$\mathbf{x}(0) = \mathbf{x}_0, \qquad \mathbf{x}(t) = \mathbf{x}. \tag{5}$$

For a nonrelativistic particle in a linear potential field with the Lagrangian $L(\mathbf{x}, \dot{\mathbf{x}}, t) = \frac{1}{2} m \dot{\mathbf{x}}^2 + \mathbf{K}.\mathbf{x}$, the equation (4) yields $\frac{d}{ds}(m\dot{\mathbf{x}}(s)) - \mathbf{K} = 0$. The trajectory minimizing the action is $\widetilde{\mathbf{x}}(s) = \mathbf{x}_0 + \frac{s}{t}(\mathbf{x} - \mathbf{x}_0) - \frac{\mathbf{K}}{2m} ts + \frac{\mathbf{K}}{2m} s^2$, and the Euler-Lagrange action is equal to $S_{cl}(\mathbf{x}, t; \mathbf{x}_0) = m\frac{(\mathbf{x}-\mathbf{x}_0)^2}{2t} + \frac{K.(\mathbf{x}+\mathbf{x}_0)}{2} t - \frac{K^2}{24m} t^3$.

More generally, in the case of a nonrelativistic particle with the Lagrangian $L(\mathbf{x}, \mathbf{v}, t) = \frac{1}{2} m \mathbf{v}^2 - V(\mathbf{x}, t)$, the Euler-Lagrange action yields the velocities of the initial and final points of the trajectory:

$$\mathbf{v}_0 = \dot{\mathbf{x}}(o) = -\frac{1}{m}\frac{\partial S_{cl}}{\partial \mathbf{x}_0}(\mathbf{x}, t; \mathbf{x}_0) \qquad and \qquad \mathbf{v}(\mathbf{x}, t; \mathbf{x}_0) = \dot{\mathbf{x}}(t) = \frac{1}{m}\frac{\partial S_{cl}}{\partial \mathbf{x}}(\mathbf{x}, t; \mathbf{x}_0). \tag{6}$$

Let us now consider that an initial action $S_0(\mathbf{x})$ is given, then *the Hamilton-Jacobi action* $S(\mathbf{x}, t)$ is the function defined by:

$$S(\mathbf{x}, t) = \min_{\mathbf{x}_0; \mathbf{u}(s), 0 \le s \le t} \left\{ S_0\,(\mathbf{x}_0) + \int_0^t L(\mathbf{x}(s), \mathbf{u}(s), s) ds \right\} \tag{7}$$

where the minimum is taken on all initial positions $\mathbf{x}_0$ and on the controls $\mathbf{u}(s)$, $s \in [0,t]$, with the state $\mathbf{x}(s)$ given by the equations (1)(2).

The introduction of the Hamilton-Jacobi action highlights the importance of the initial action $S_0(\mathbf{x})$, while texbooks do not well differentiate these two actions.

Noting that $S_0(\mathbf{x}_0)$ does not play a role in (7) for the minimization on $\mathbf{u}(s)$, we obtain a new relation between the Hamilton-Jacobi action and Euler-Lagrange action:

$$S(\mathbf{x},t) = \min_{\mathbf{x}_0}(S_0(\mathbf{x}_0) + S_{cl}(\mathbf{x},t;\mathbf{x}_0)). \tag{8}$$

It is an equation similar to the Hopf-Lax or Lax-Oleinik formula (Evans (1998)).

For a particle in a linear potential $V(\mathbf{x}) = -\mathbf{K}.\mathbf{x}$ with the initial action $S_0(\mathbf{x}) = m\mathbf{v}_0 \cdot \mathbf{x}$, we deduce of the equation (8) that the Hamilton-Jacobi action is equal to $S(\mathbf{x},t) = m\mathbf{v}_0 \cdot \mathbf{x} - \frac{1}{2}m\mathbf{v}_0^2 t + \mathbf{K}.\mathbf{x}t - \frac{1}{2}\mathbf{K}.\mathbf{v}_0 t^2 - \frac{\mathbf{K}^2 t^3}{6m}$.

For the Lagrangian $L(\mathbf{x},\dot{\mathbf{x}},t) = \frac{1}{2}m\dot{\mathbf{x}}^2 - V(\mathbf{x},t)$, we deduce the well-known result (Evans (1998)):

The velocity of a non-relativistic classical particle in a potential field is given for each point ($\mathbf{x}$,t) *by*:

$$\mathbf{v}(\mathbf{x},t) = \frac{\nabla S(\mathbf{x},t)}{m} \tag{9}$$

where $S(\mathbf{x},t)$ *is the Hamilton-Jacobi action, a solution to the Hamilton-Jacobi equations:*

$$\frac{\partial S}{\partial t} + \frac{1}{2m}(\nabla S)^2 + V(\mathbf{x},t) = 0 \tag{10}$$

$$S(\mathbf{x},0) = S_0(\mathbf{x}). \tag{11}$$

Equation (9) shows that the solution $S(\mathbf{x},t)$ of the Hamilton-Jacobi equations yields the velocity field for each point $(\mathbf{x},t)$ from the velocity field $\frac{\nabla S_0(\mathbf{x})}{m}$ at initial time. In particular, if at initial time, we know the initial position $\mathbf{x}_{init}$ of a particle, its velocity at this time is equal to $\frac{\nabla S_0(\mathbf{x}_{init})}{m}$. From the solution $S(\mathbf{x},t)$ of the Hamilton-Jacobi equations, we deduce with (9) the trajectories of the particle. The Hamilton-Jacobi action $S(\mathbf{x},t)$ is then a field which "pilots" the particle.

3. Interpretation of the Euler-Lagrange and Hamilton-Jacobi actions

It is difficult to interpret directly the equations (3) and (7). The equation (3) seems to show that, among the trajectories which can reach $(\mathbf{x}, t)$ from the initial position $\mathbf{x}_0$, Nature chooses the velocity at each time which yields the minimum (or the extremum) of the Euler-lagrange action. The equation (7) seems to show that, among the trajectories which can reach $(\mathbf{x}, t)$ from an unknown initial position and a known initial velocity field, Nature chooses the initial position and at each time the velocity which yields the minimum (or the extremum) of the Hamilton-Jacobi action.

It is much easier to interpret the Euler-Lagrange equations (4,5,6) and the Hamilton-Jacobi equations (9,10,11).

The equations (9,10,11) show that the Hamilton-Jacobi action $S(\mathbf{x}, t)$ does not solve only a given problem with a single initial condition $\left(\mathbf{x}_0, \frac{\nabla S_0(\mathbf{x}_0)}{m}\right)$, but a set of problems with an infinity of initial conditions, all the pairs $\left(\mathbf{y}, \frac{\nabla S_0(\mathbf{y})}{m}\right)$. It answers the following question: "If we know the action (or the velocity field) at the initial time, can we determine the action (or the velocity field) at each later time?" This problem is solved sequentially by the (local) evolution equation (10). This is an *a priori* point of view. It is the problem solved by Nature with the principle of least action.

Without knowing the initial velocity, the Euler-Lagrange action answers a problem posed by the observer, and not by Nature: "If a particle in $\mathbf{x}_0$ at the initial time reachs $\mathbf{x}$ at time t, what was its initial velocity $\mathbf{v}_0$?" The resolution of this problem implies that the observer solves the Euler-Lagrange equations (4,5). Unfortunately, this set of equations are quite involved, for they necessitate the study of the whole trajectory. We have seen that this velocity is given by equation (6): $\mathbf{v}_0 = -\frac{1}{m}\frac{\partial S_{cl}}{\partial \mathbf{X}_0}(\mathbf{x}, t; \mathbf{x}_0)$. This is an *a posteriori* point of view.

We are now in a position to answer the Poincar's puzzle: the Hamilton-Jacobi action does not use the "final causes" and seems to be the action used by Nature; the Euler-Lagrange action uses the "final causes" and is the action used by an observer to determine retrospectively the trajectory of the particle and its initial velocity.

4. Aknowledgements

I am grateful to Sebastien Lepaul and Yohan Pelosse for their insightful comments.

References

P. L. de Maupertuis, Accord de différentes lois de la nature qui avaient jusqu'ici paru incompatibles, Histoire de l'Académie Royale des Sciences [de Paris], Mémoires de Mathématiques et de Physique (1744) 417–426.

P. L. de Maupertuis, Les Loix du mouvement et du repos déduites d'un principe métaphysique, Histoire de l'Académie Royale des Sciences et des Belles Lettres [de Berlin] (1746) 267–294.

L. Euler, Methodus Inveniendi Lineas Curvas Maximi Minive Proprietate Gaudentes, Bousquet, Lausanne et Geneva. reprint in Leonhardi Euleri Opera Omnia: Series I vol 24 (1952) C. Cartheodory (ed.) Orell Fuessli,Zurich., 1744.

J. L. Lagrange, Analytic Mechanics, Gauthier-Villars, Paris, 1888, 2nd ed., translated by V. Vagliente and A. Boissonade (Klumer Academic, Dordrecht, 2001), 1888.

W. R. Hamilton, On a general method in dynamics, by which the study of the motions of all free systems of attracting or repelling points is reduced to the search and differentiation of one central Relation or characteristic Function, Philosophical Transactions of the Royal Society of London II (1834) 247–308.

W. R. Hamilton, Second essay on a general method in dynamics, Philosophical Transactions of the Royal Society of London I (1835) 95–144.

C. G. J. Jacobi, Vorlesungen über Dynamik, Reimer, Berlin, 1866.

R. P. Feynman, R. B. Leighton, M. Sands, The Feynman Lectures on Physics, vol. II, Addison-Wesley, Reading, MA, 1964, 1964.

L. D. Landau, E. M. Lifshitz, Mechanics, Course of Theoretical Physics, vol. 1, Buttreworth-Heinemann, London, 1976, 3rd ed., 1957.

H. Poincaré, La Science et l'Hypothèse, Flammarion, translated in The Foundations of Sciences: Science and Hypothesis, The value of Science, Science and Method, New York: Science Press, 1913., 1902.

L. C. Evans, Partial Differential Equations, Graduate Studies in Mathematics 19, American Mathematical Society, 1998.